Features of Hadron Structure with Basis Light-Front Quantization

Chandan Mondal

Institute of Modern Physics, Chinese Academy of Sciences, Lanzhou, China

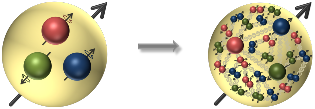

in collaboration with

Jiangshan Lan, Jialin Chen, Jiatong Wu, Ziqi Zhang, Zhi Hu, Siqi Xu, Xingbo Zhao, Yang Li and James P. Vary

May 9, 2022

Jefferson Lab

Overview

Introduction

Basis Light-Front Quantization (BLFQ) Approach to

- Mesons
  - BLFQ-NJL Model
  - With One Dynamical Gluon
- Nucleon
  - Leading Fock-Sector
  - With One Dynamical Gluon

Conclusions

Mass & Spin

- About 99% of the visible mass is contained within nuclei
- Nucleon: composite particles, built from nearly massless quarks (~ 1% of the nucleon mass) and gluons
- *How does 99% of the nucleon mass emerge?*
- Quantitative decomposition of *nucleon spin* in terms of quark and gluon degrees of freedom is not yet fully understood.
- *To address these fundamental issues → nature of the subatomic force between quarks and gluons, and the internal landscape of nucleons.*

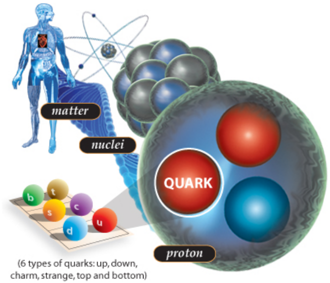

[1]

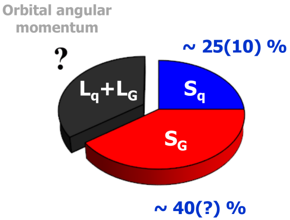

[1] Andrea Signori, University of Pavia and Jefferson Lab

Hadron Tomography

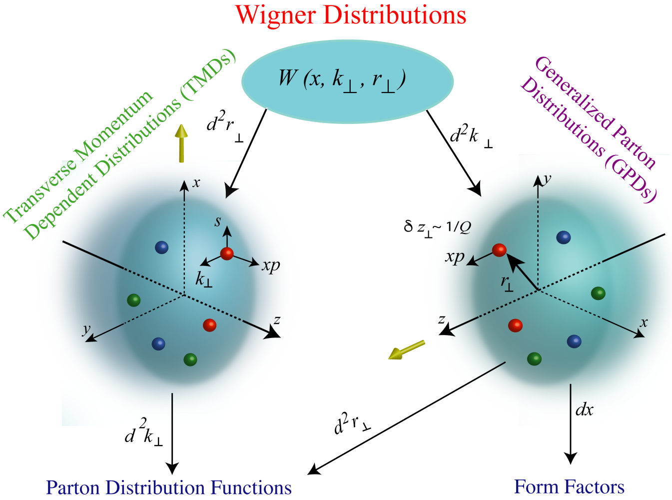

- $x \to$ longitudinal momentum fraction; $k_\perp \to$ parton transverse momentum; $r_\perp \to$ transverse distance from the center.

Form Factors Vs PDFs Vs GPDs

Elastic Scattering

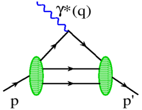

Deep Inelastic Scattering

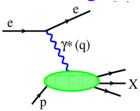

Deeply virtual Compton Scattering

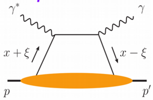

Established extended nature of nucleon

discovered the existence (quarks) inside the nucleon

provides 3D spatial structure of the nucleon

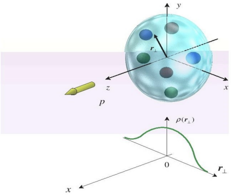

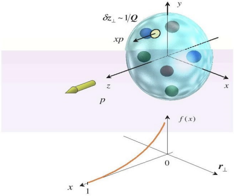

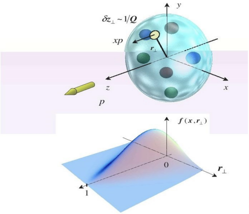

charge and magnetization distribution

longitudinal momentum distribution

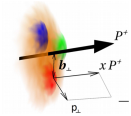

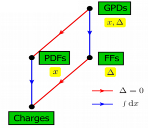

Basis Light-Front Quantization (BLFQ)

A computational framework for solving relativistic many-body bound state problems in quantum field theories [1]

$$P^- P^+ |\Psi\rangle = M^2 |\Psi\rangle$$

- $P^- \equiv P^0 - P^3$: light-front Hamiltonian
- $P^+ \equiv P^0 + P^3$: longitudinal momentum
- $|\Psi\rangle$ mass eigenstate
- M^2 : mass squared eigenvalue for eigenstate $|\Psi\rangle$
- First-principle / effective Hamiltonian as input
- Evaluate observables

$$O \sim \langle \Psi | \hat{O} | \Psi \rangle$$

- direct access to light-front wavefunction of bound states

GOAL

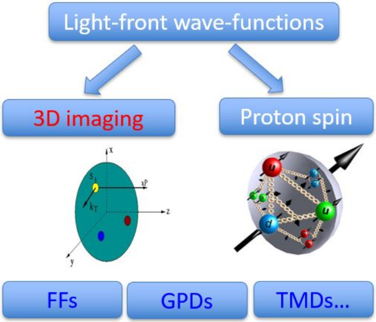

[1] Vary, Honkanen, Li, Maris, Brodsky, Harindranath, *et. al.*, Phys. Rev. C 81, 035205 (2010).

Solution proposed by BLFQ

Discrete basis and their direct product	Truncation
2D HO $\phi_{nm}(p^{\perp})$ in the transverse plane	$\sum_i (2n_i + \lvert m_i \rvert + 1) \leq N_{\max}$
Plane-wave in the longitudinal direction	$\sum_i k_i = K, \quad x_i = \frac{k_i}{K}$
Light-front helicity state for spin d.o.f.	$\sum_i (m_i + \lambda_i) = M_J$
$\alpha_i = (k_i, n_i, m_i, \lambda_i)$ $\lvert\alpha\rangle = \otimes_i \lvert\alpha_i\rangle$	Fock sector truncation

- Fock expansion of hadronic bound states:

$$|\text{Meson}\rangle = \psi_{(q\bar{q})}|q\bar{q}\rangle + \psi_{(q\bar{q}+q\bar{q})}|q\bar{q}q\bar{q}\rangle + \psi_{(q\bar{q}+1g)}|q\bar{q}g\rangle + \dots\,,$$

$$|\text{Baryon}\rangle = \psi_{(3q)}|qqq\rangle + \psi_{(3q+q\bar{q})}|qqqq\bar{q}\rangle + \psi_{(3q+1g)}|qqqg\rangle + \dots\,,$$

[1] Vary, Honkanen, Li, Maris, Brodsky, Harindranath, *et. al.*, Phys. Rev. C 81, 035205 (2010).

Applications of BLFQ

QCD systems

- Heavy mesons: spectrum, decay constant, elastic form factor, radii, radiative transitions, distribution amplitude, PDFs, GPDs

—Li, Chen, Zhao, Maris, Vary, Adhikari, M Li, Tang, A El-Hady, Lan, Wu, CM (2016 - 2022)

- Light mesons: spectrum, decay constant, elastic form factor, radii, distribution amplitude, PDFs, GPDs, TMDs

—Jia, Vary, Lan, Zhao, Qian, Li, Fu, J. Chen, Wu, CM (2018 - 2022)

- Baryons: EMFFs, axial form factor, radii, PDFs, GPDs, TMDs, OAM

—Xu, Hu, Peng, Zhu, Zhao, Li, Chakrabarti, Vary, Lan, Liu, CM (2019-2022)

- Tetraquarks: Masses of all-charm tetraquarks

—Kuang, Serafin, Zhao, Vary (2022)

QED systems

- Electron: anomalous magnetic moments, GPDs
- positronium: wave function, spectroscopy, FFs, GPDs
- Photon: wave function, structure functions, GPDs, TMDs

—Zhao, Wiecki, Li, Honkanen, Maris, Vary, Brodsky, Fu, Hu, Nair, CM (2013 - 2022)

Effective Hamiltonian : BLFQ-NJL Model

$$|\,\pi\rangle_{\text{phys}} = a\,|\,q\bar{q}\rangle + b\,|\,q\bar{q}g\rangle + c\,|\,q\bar{q}q\bar{q}\rangle + \ldots$$

kinetic energy

transverse confining potential [2]

$$H_{\text{eff}} = \frac{\vec{k}^{\perp 2}+m_q^2}{x} + \frac{\vec{k}^{\perp 2}+m_{\bar{q}}^2}{1-x} + \kappa^4 x(1-x)\vec{r}^{\perp 2}$$

$$+ \frac{\kappa^4}{(m_q+m_{\bar{q}})^2}\partial_x\big(x(1-x)\partial_x\big) + H_{\text{NJL}}^{\text{eff}}$$

longitudinal confining potential [3]

Nambu–Jona-Lasinio (NJL) interaction [4]

1 Jia and Vary, Phys. Rev. C 99, 035206 (2019)
2 Brodsky, Teramond, Dosch and Erlich, Phys. Rep. 584, 1 (2015).
3 Li, Maris, Zhao and Vary, Phys. Lett. B 758, 118 (2016)
4 Klimt, Lutz, Vogl and Weise, Nucl. Phys. A **516**, 429-468 (1990).

Meson Light-Front Wave Functions (LFWFs)

- Valence LFWFs in orthonormal bases

$$\psi_{rs}(x,\vec{\kappa}^{\perp}) = \sum_{n,m,l} \langle n,m,l,r,s|\psi\rangle \times \phi_{nm}\left(\vec{\kappa}^{\perp}\right)\chi_l(x)$$

- Transverse direction (2D-HO)

$$\phi_{nm}\left(\vec{\kappa}^{\perp}\right) \sim \left(|\vec{\kappa}^{\perp}|\right)^{|m|} \times \exp\left(-\vec{\kappa}^{\perp 2}\right) L_n^{|m|}\left(\vec{\kappa}^{\perp 2}\right); \quad 0 \le n \le N_{\max}$$

- Longitudinal direction (Jacobi polynomial basis)

$$\chi_l(x) \sim x^{\beta/2}(1-x)^{\alpha/2} P_l^{(\alpha,\beta)}(2x-1); \qquad 0 \le l \le L_{\max}$$

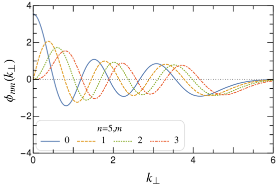

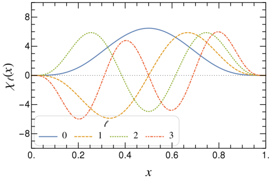

- Coefficients $\langle n,m,l,r,s|\psi\rangle$: eigenvector in BLFQ basis representation.

[2] Li, Maris, and Vary, Phys. Rev. D 96 , 016022 (2017)

BLFQ-NJL Model Parameters

- Parameters are fixed to
  - reproduce ground state masses
  - experimental charge radii of π^+ and K^+ [1]
- Successfully applied to
  - compute PDAs and EMFFs [1]
  - PDFs for pion and kaon and pion-nucleus induced Drell-Yan cross sections [2][3]
  - GPDs [4]
- Summary of model parameters

Valence flavor	$N_{\max}$	$L_{\max}$	κ(MeV)	m_q(MeV)	$m_{\bar{q}}$(MeV)
$u\bar{d}$	8	8–32	227	337	337
$u\bar{s}$	8	8–32	276	308	445

[1] Jia and Vary, Phys. Rev. C 99, 035206 (2019)
[2] Lan, CM, Jia, Zhao, Vary, Phys. Rev. Lett. 122 172001 (2019)
[3] Lan, CM, Jia, Zhao, Vary, Phys. Rev. D 101, 034024 (2020)
[4] Adhikari, CM, Nair, Xu, Jia, Zhao and Vary, Phys. Rev. D 104, 114019 (2021)

Applications: Light Meson PDFs

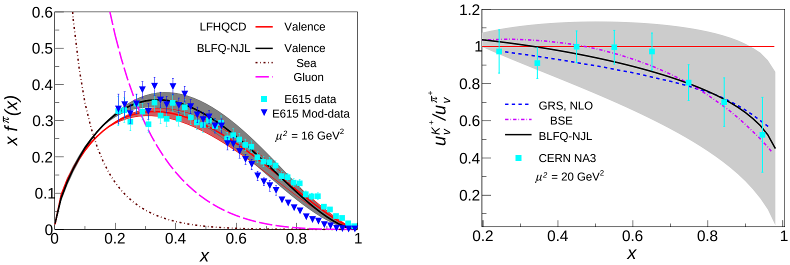

Light-front effective Hamiltonian, $H_{\rm eff}$: ($\mu^2_{0\pi} = 0.240 \pm 0.024$ GeV^2)

Diagonalizing $H_{\rm eff}$ ⇒ LF wavefunction ⇒ Initial PDFs ⇒ Scale evolution [1].

$$\psi_{rs}(x, \vec{\kappa}^\perp) = \sum_{n,m,l} \langle n, m, l, r, s|\psi\rangle \times \phi_{nm}\left(\vec{\kappa}^\perp\right)\chi_l(x)$$

- 2D-HO $\phi_{nm}\left(\vec{\kappa}^\perp\right)$ in the transverse plane.
- Jacobi polynomial basis $\chi_l(x)$ in the longitudinal direction.

[1] Lan, CM, Jia, Zhao, Vary, Phys. Rev. Lett. 122 172001 (2019)

Moments of Pion PDF

Moments of the valence quark PDF

$$\langle x^n \rangle = \int_0^1 dx\ x^n f_v^\pi(x, \mu^2),\ \ n = 1, 2, 3, 4.$$

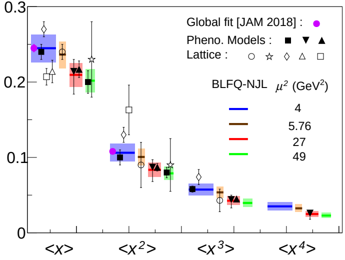

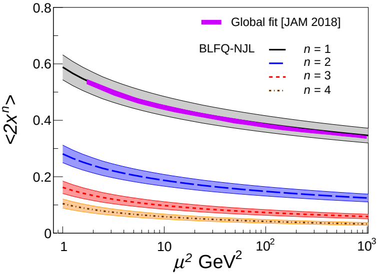

Consistent with global fit, lattice QCD, and phenomenological models.

[1] Lan, CM, Jia, Zhao, Vary, Phys. Rev. D 101, 034024 (2020)

Distribution Amplitude

DAs of pseudoscalar states

$$\phi(x,\mu_0) \sim \frac{1}{\sqrt{x(1-x)}} \int \frac{d^2\vec{k}_\perp}{2(2\pi)^3} \frac{(\psi_{\uparrow\downarrow} - \psi_{\downarrow\uparrow})}{\sqrt{2}}$$

- DA evolution: ERBL equations (Gegenbauer basis)

  Ruiz, *et. al.* PRD 66, (2002)
- Oscillations → Basis artifacts
- With increasing $L_{\max}$ the DA tends toward a smooth function
- Our DA is close to Asymptotic DA

Decay constant f_π:

BLFQ (Basis $[8,32]$): 145.3 MeV

Experimental data: 130.2 ± 1.7 MeV

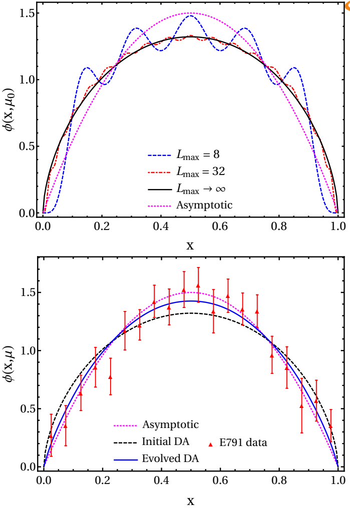

- Consistent with the FNAL-E-791

[1] Mondal, Nair, Jia, Zhao and Vary, Phys. Rev. D 104, 094034 (2021)

$\pi \to \gamma^* \gamma$ Transition Form Factor

$$\langle \gamma(P-q)|J^\mu|M(P)\rangle = -ie^2 F_{M\gamma}(Q^2)\epsilon^{\mu\nu\rho\sigma} P_\nu \epsilon_\rho q_\sigma \,,$$

- Results for $\{N_{\max}, L_{\max}\} \equiv \{8, 8\}$, $\{8, 16\}$, and $\{8, 32\}$ (upper panel)
- The results show a good convergence trend over the range of Q^2
- Consistent with data reported by Belle Collaboration.
- Deviates from the rapid growth of the large Q^2 data reported by BaBar Collaboration.

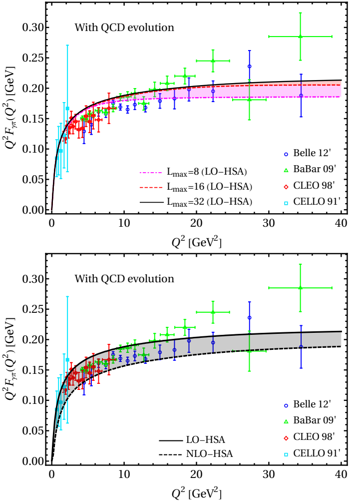

[1] Mondal, Nair, Jia, Zhao and Vary, Phys. Rev. D 104, 094034 (2021)

Effective Hamiltonian with One Dynamical Gluon

[Lan, et al, PRL 19']

$$|\text{meson}\rangle = |q\bar{q}\rangle + \cdots$$

One step forward

[Lan, Fu, Mondal, Zhao, Vary, Phys. Lett. B 825 (2022) 136890]

$$|\text{meson}\rangle = a|q\bar{q}\rangle + b|q\bar{q}g\rangle + \cdots$$

H_{int}	$\lvert q\bar{q}\rangle$	$\lvert q\bar{q}g\rangle$
$\langle q\bar{q}\rvert$	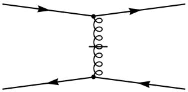	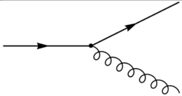
$\langle q\bar{q}g\rvert$	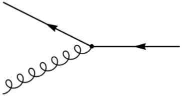	0

$$H_{\text{eff}} = \frac{\vec{k}_\perp^2 + m_q^2}{x} + \frac{\vec{k}_\perp^2 + m_{\bar{q}}^2}{1-x} + \kappa^4 x(1-x)\vec{r}_\perp^2 - \frac{\kappa^4}{(m_q + m_{\bar{q}})^2}\partial_x(x(1-x)\partial_x) + H_{\text{eff}}^{\text{NJL}}$$

$$P^- = \frac{\vec{k}_\perp^2 + m_q^2}{x} + \frac{\vec{k}_\perp^2 + m_{\bar{q}}^2}{1-x} + \kappa^4 x(1-x)\vec{r}_\perp^2 - \frac{\kappa^4}{(m_q + m_{\bar{q}})^2}\partial_x(x(1-x)\partial_x) + H_{\text{int}}$$

5

Light-Front QCD Hamiltonian

[Brodsky et al, 1998]

$$P_{-,LFQCD} = \frac{1}{2}\int d^3x\, \bar{\psi}\gamma^+ \frac{(i\partial^\perp)^2 + m^2}{i\partial^+}\,\psi - \frac{1}{2}\int d^3x\, A^i_a (i\partial^\perp)^2 A^i_a$$

$$+g\int d^3x\, \bar{\psi}\gamma_\mu A^\mu\, \psi$$

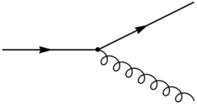

$$+\frac{1}{2}g^2\int d^3x\, \bar{\psi}\gamma_\mu A^\mu \frac{\gamma^+}{i\partial^+}\gamma_\nu A^\nu \psi$$

$$-ig^2\int d^3x\, f^{abc}\bar{\psi}\gamma^+ T^c\psi \frac{1}{(i\partial^+)^2}(i\partial^+ A^\mu_a A_{\mu b})$$

$$+\frac{1}{2}g^2\int d^3x\, \bar{\psi}\gamma^+ T^a\psi \frac{1}{(i\partial^+)^2}\bar{\psi}\gamma^+ T^a\psi$$

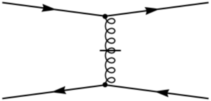

$$+ig\int d^3x\, f^{abc} i\partial^\mu A^{\nu a} A^b_\mu A^c_\nu$$

$$-\frac{1}{2}g^2\int d^3x\, f^{abc} f^{ade}\, i\partial^+ A^\mu_b A_{\mu c} \frac{1}{(i\partial^+)^2}(i\partial^+ A^+_d A_{\nu e})$$

$$+\frac{1}{4}g^2\int d^3x\, f^{abc} f^{ade} A^\mu_b A^\nu_c A_{\mu d} A_{\nu e}.$$

Mass Spectrum of Light Unflavored Mesons

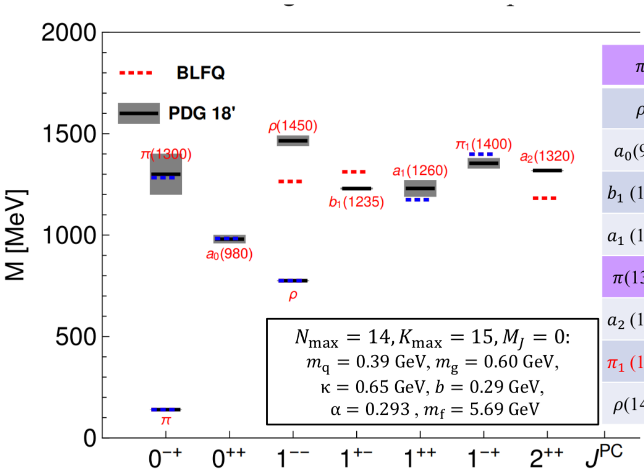

	Norm$q\bar{q}$	DC [MeV]
π	0.492	151
ρ	0.486	141
$a_0(980)$	0.370	0
b_1 (1235)	0.30	0
a_1 (1260)	0.324	13
$\pi(1300)$	0.284	59
a_2 (1320)	0.320	0
π_1 (1400)	0.002	0
$\rho(1450)$	0.312	50

$|\text{meson}\rangle = a|q\bar{q}\rangle + b|q\bar{q}g\rangle + \cdots$

Fix the parameters by fitting six blue states

- $\pi_1(1400)$: $|q\bar{q}g\rangle$ dominates
- $\pi(1300)$: the DC is smaller than the DC of pion

[1] J. Lan, K. Fu, CM, X. Zhao and J. P. Vary, Phys.Lett.B 825 (2022)

Pion Wavefunction with Leading Fock Sector

$$\Psi^{\mathcal{N},M_J}_{\{x_i,\vec{p}^2_{\perp i},\lambda_i\}} = \sum_{\{n_i m_i\}} \psi^{\mathcal{N}}(\{\bar{\alpha}_i\}) \prod_{i=1}^{\mathcal{N}} \phi_{n_i m_i}(\vec{p}_{\perp i}, b)$$

$$|\pi\rangle = a|q\bar{q}\rangle + b|q\bar{q}g\rangle + \cdots$$

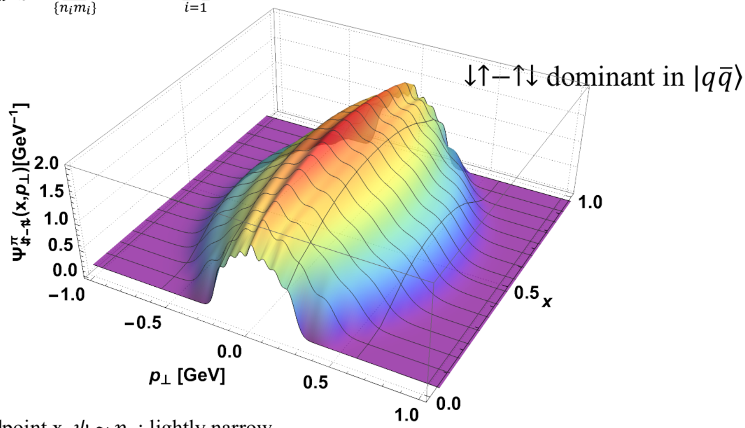

- At endpoint x, $\psi \sim p_\perp$: lightly narrow
- At middle x, $\psi \sim p_\perp$: a little bit wide

8

Pion Electromagnetic Form Factor

$$\langle \Psi(p') | J^+_{\rm EM} | \Psi(p) \rangle = (p + p')^+ F(Q^2)$$

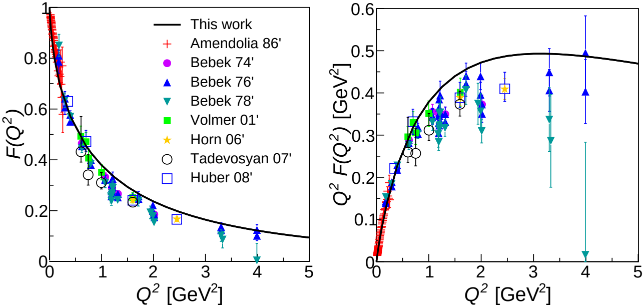

- $N_{\rm max} = 14$ (BLFQ basis), implies the UV regulator $\Lambda_{\rm UV} \approx 1$ GeV.
- Reasonable agreement with experimental data ($Q^2 < 1$).
- $F(Q^2) \sim 1/Q^2$ at large Q^2.

[1] J. Lan, K. Fu, CM, X. Zhao and J. P. Vary, Phys.Lett.B 825 (2022)

Pion PDFs at Model Scale

$$f_i(x) = \sum_{\mathcal{N},\lambda_i} \int [d\mathcal{X} d\mathcal{P}^\perp]_\mathcal{N} \left| \psi^{\mathcal{N},M_j=0}_{\{x_i,\vec{p}^2_{\perp i},\lambda_i\}} \right|^2 \delta(x - x_i)$$

$$|\pi\rangle = a|q\bar{q}\rangle + b|q\bar{q}g\rangle + \cdots$$

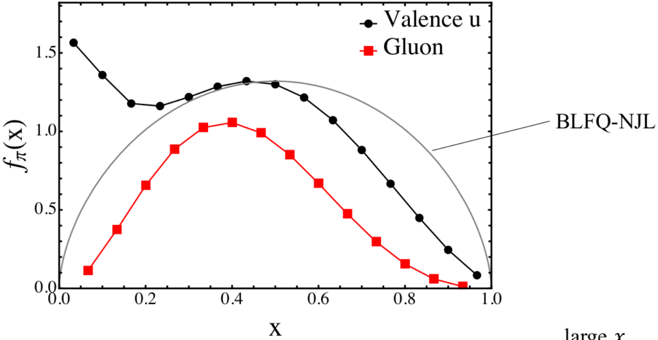

			large x
$\mu^2_{0\mathrm{BLFQ-NJL}} = 0.240\ \mathrm{GeV}^2$	$\langle x\rangle_{\mathrm{gluon}} = \mathbf{0}$;	$\langle x\rangle_{\mathrm{valence}\ u} = \mathbf{0.5}$	$(1-x)^{0.596}$
$\mu^2_{0\mathrm{BLFQ}} = 0.34\ \mathrm{GeV}^2$	$\langle x\rangle_{\mathrm{gluon}} = \mathbf{0.216}$;	$\langle x\rangle_{\mathrm{valence}\ u} = \mathbf{0.392}$	$(1-x)^{1.4}$

Pion PDFs after QCD Evolution

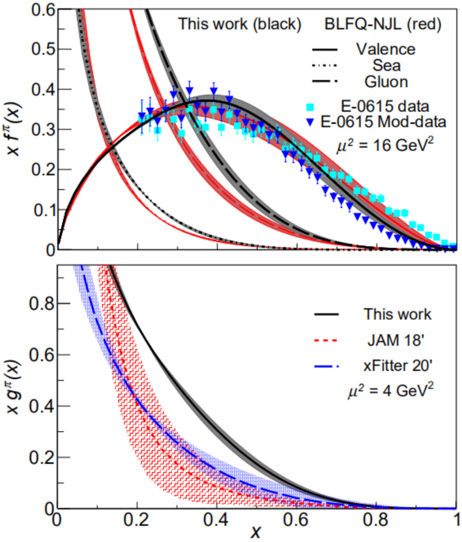

$$|\pi\rangle = a|q\bar{q}\rangle + b|q\bar{q}g\rangle + \dots$$

- Large-x behavior $(1-x)^{1.77}$ close to PQCD prediction
- Gluon distribution increases

$\langle x\rangle$ @ 4 GeV^2	Valence	Gluon	Sea
BLFQ	**0.483**	**0.421**	**0.096**
BLFQ-NJL	0.489	0.398	0.113
[BSE 2019']	0.48(3)	0.41(2)	0.11(2)

[1] J. Lan, K. Fu, CM, X. Zhao and J. P. Vary, Phys.Lett.B 825 (2022)

Pion GPDs

[M. Diehl, Phys. Rep. 388 (2003) 41-277]

$$|\pi\rangle = a|q\bar{q}\rangle + b|q\bar{q}g\rangle + \dots$$

$$H_\pi^q(x, \xi = 0, t) = \frac{1}{2}\int \frac{dz^-}{2\pi} e^{ixP^+z^-} \left\langle \pi, P + \frac{\Delta}{2}\middle| \bar{q}\left(-\frac{z}{2}\right)\gamma^+ q\left(\frac{z}{2}\right)\middle|\pi, P - \frac{\Delta}{2}\right\rangle_{\substack{z^+=0\\ z_\perp=0}}$$

$$H_\pi^g(x, \xi = 0, t) = \frac{1}{P^+}\int \frac{dz^-}{2\pi} e^{ixP^+z^-} \left\langle \pi, P + \frac{\Delta}{2}\middle| G^{+\mu}\left(-\frac{z}{2}\right) G_\mu^+\left(\frac{z}{2}\right)\middle|\pi, P - \frac{\Delta}{2}\right\rangle_{\substack{z^+=0\\ z_\perp=0}}$$

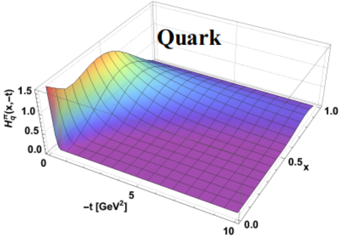

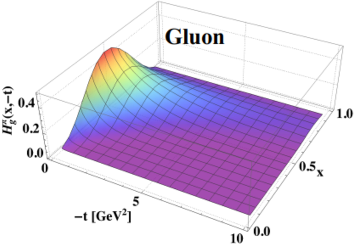

- Quark content enhanced at small x with $|q\bar{q}g\rangle$
- Falls slowly at larger x
- Emerge at larger x range for larger $-t$

Preliminary

[1] J. Lan, J. Wu, et al., in preparation

Pion GPDs in Impact Parameter Space

[M. Diehl, Phys. Rep. 388 (2003) 41-277]

$$|\pi\rangle = a|q\bar{q}\rangle + b|q\bar{q}g\rangle + \ldots$$

$$H_\pi^q(x,\xi=0,t) = \frac{1}{2}\int \frac{dz^-}{2\pi} e^{ixP^+z^-} \left\langle \pi, P+\frac{\Delta}{2} \middle| \bar{q}\left(-\frac{z}{2}\right)\gamma^+ q\left(\frac{z}{2}\right) \middle| \pi, P-\frac{\Delta}{2} \right\rangle_{\substack{z^+=0\\ z_\perp=0}}$$

$$H_\pi^g(x,\xi=0,t) = \frac{1}{P^+}\int \frac{dz^-}{2\pi} e^{ixP^+z^-} \left\langle \pi, P+\frac{\Delta}{2} \middle| G^{+\mu}\left(-\frac{z}{2}\right) G_\mu^+\left(\frac{z}{2}\right) \middle| \pi, P-\frac{\Delta}{2} \right\rangle_{\substack{z^+=0\\ z_\perp=0}}$$

FT → The impact parameter distributions (IPDs)

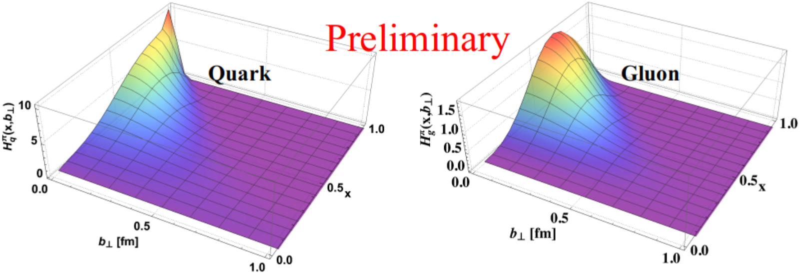

[1] J. Lan, J. Wu, *et. al.*, in preparation

x-Dependent Square Radius

$$|\pi\rangle = a|q\bar{q}\rangle + b|q\bar{q}g\rangle + \dots$$

x-dependent squared radius

$$\langle b_\perp^2\rangle^{q,g}(x) = \frac{\int d^2\mathbf{b}_\perp \mathbf{b}_\perp^2 H_\pi^{q,g}(x,\mathbf{b}_\perp)}{\int d^2\mathbf{b}_\perp H_\pi^{q,g}(x,\mathbf{b}_\perp)}$$

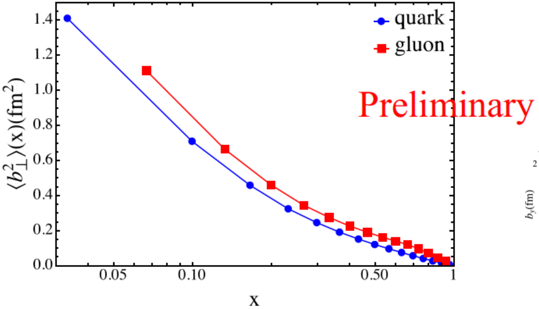

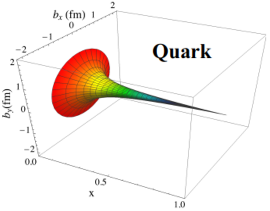

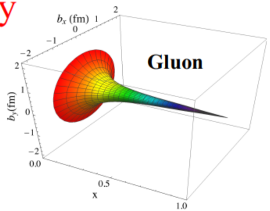

- The gluon is slightly broader than the quark

[1] J. Lan, J. Wu, *et. al.*, in preparation

Pion TMDs

[Boer & Mulders PRD 57 (1998) 5780]
[Pasquini et al, PRD 90 (2014) 014050]

$$|\pi\rangle = a|q\bar{q}\rangle + b|q\bar{q}g\rangle + \ldots$$

$$f_1^q(x,k_\perp) = \frac{1}{2}\int \frac{dz^- d^2 z_\perp}{(2\pi)^3} e^{i(z^- k^+ - z_\perp k_\perp)} \left\langle \pi, P\left|\bar{q}\left(-\frac{z}{2}\right)\gamma^+ q\left(\frac{z}{2}\right)\right|\pi, P\right\rangle_{z^+=0}$$

$$f_1^g(x,k_\perp) = \frac{1}{xP^+}\int \frac{dz^- d^2 z_\perp}{(2\pi)^3} e^{i(z^- k^+ - z_\perp k_\perp)} \left\langle \pi, P\left|G^{+\mu}\left(-\frac{z}{2}\right)G_\mu^+\left(\frac{z}{2}\right)\right|\pi, P\right\rangle_{z^+=0}$$

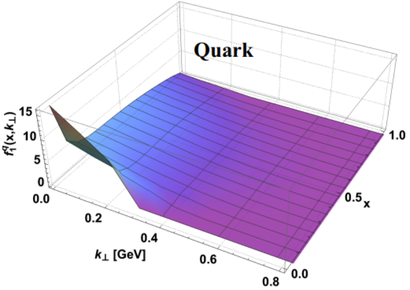

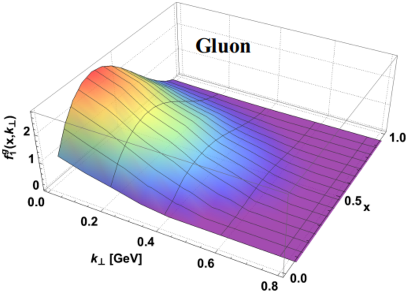

- The TMD decreases with $k_\perp$
- Vanishes after $k_\perp \sim 0.7$ GeV

Preliminary

[1] J. Lan, J. Wu, *et. al.*, in preparation

Strange Meson Mass Spectrum

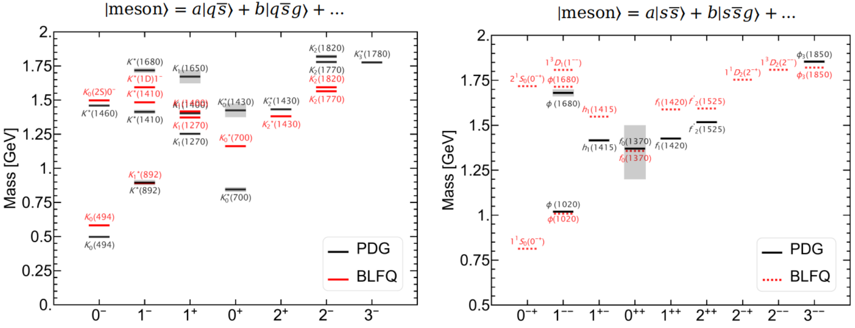

$N_{\max} = 14, K_{\max} = 15,\ M_J = 0$:
$m_q = 0.39$ GeV, $m_s = 0.64$ GeV, $m_g = 0.60$ GeV,
$\kappa = 0.65$ GeV, $b = 0.29$ GeV,
$\alpha = 0.293$, $m_f = 5.69$ GeV

$N_{\max} = 14, K_{\max} = 15,\ M_J = 0$:
$m_s = 0.64$ GeV, $m_g = 0.60$ GeV,
$\kappa = 0.65$ GeV, $b = 0.29$ GeV,
$\alpha = 0.293$, $m_f = 5.69$ GeV

[Lan, et al, Phys. Lett. B 825 (2022) 136890]

[1] J. Chen *et. al.*, in preparation

Wavefunction in Leading Fock Sector

$$\Psi^{\mathcal{N},M_J}_{\{x_i,\vec{p}^2_{\perp i},\lambda_i\}} = \sum_{\{n_i m_i\}} \psi^{\mathcal{N}}(\{\overline{\alpha}_i\}) \prod_{i=1}^{\mathcal{N}} \phi_{n_i m_i}(\vec{p}_{\perp i}, b)$$

$|\text{meson}\rangle = a|q\bar{s}\rangle + b|q\bar{s}g\rangle + \ldots$

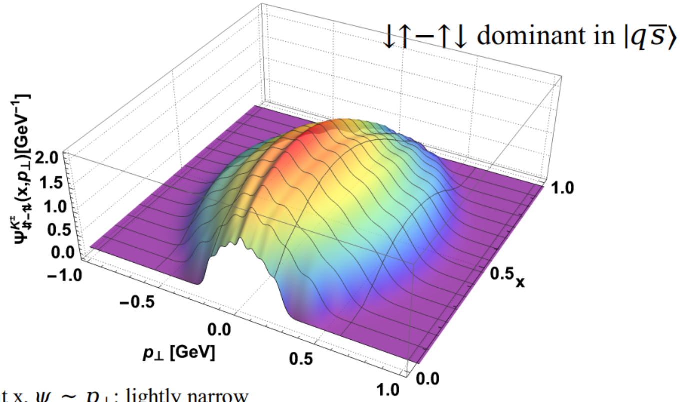

- At endpoint x, $\psi \sim p_\perp$: lightly narrow
- At middle x, $\psi \sim p_\perp$: a little bit wide
- The peak slightly less than x=1/2

Kaon Electromagnetic Form Factor

$$\langle\Psi(p')|J^+_{\rm EM}|\Psi(p)\rangle = (p+p')^+F(Q^2)$$

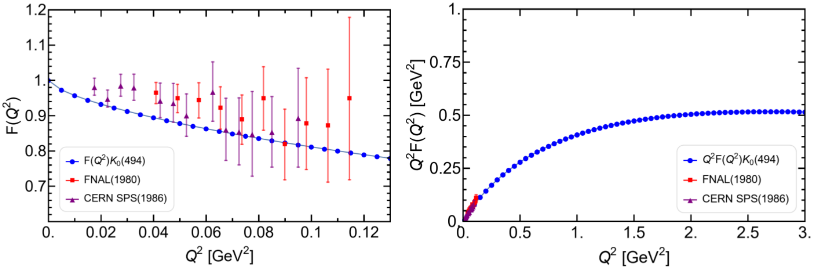

- Reasonable agreement with experimental data.
- $F(Q^2) \sim 1/Q^2$ at large Q^2.

[1] J. Chen *et. al.*, in preparation

Kaon GPDs

[M. Diehl, Phys. Rep. 388 (2003) 41-277]

$$|\mathrm{K}\rangle = a|q\bar{s}\rangle + b|q\bar{s}g\rangle + \ldots$$

$$H_K^q(x,\xi=0,t) = \frac{1}{2}\int\frac{dz^-}{2\pi}e^{ixP^+z^-}\left\langle K, P+\frac{\Delta}{2}\middle|\bar{q}\left(-\frac{z}{2}\right)\gamma^+ q\left(\frac{z}{2}\right)\middle|K, P-\frac{\Delta}{2}\right\rangle_{\substack{z^+=0\\ z_\perp=0}}$$

$$H_K^g(x,\xi=0,t) = \frac{1}{P^+}\int\frac{dz^-}{2\pi}e^{ixP^+z^-}\left\langle K, P+\frac{\Delta}{2}\middle|G^{+\mu}\left(-\frac{z}{2}\right)G_\mu^+\left(\frac{z}{2}\right)\middle|K, P-\frac{\Delta}{2}\right\rangle_{\substack{z^+=0\\ z_\perp=0}}$$

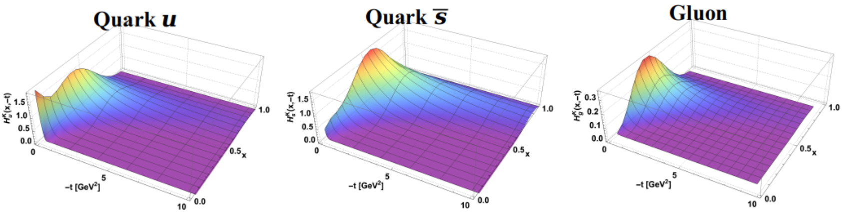

- Quark u content enhanced at small x with $|q\bar{s}g\rangle$
- Falls slowly at larger x
- Emerge at larger x range for larger $-t$

Preliminary

[1] J. Chen *et. al.*, in preparation

Nucleon within BLFQ

- The LF eigenvalue equation: $H_{\text{eff}}|\Psi\rangle = M^2|\Psi\rangle$

$$H_{\text{eff}} = \sum_a \frac{\vec{p}_{\perp a}^2 + m_a^2}{x_a} + \frac{1}{2}\sum_{a\neq b}\kappa^4\left[x_a x_b(\vec{r}_{\perp a} - \vec{r}_{\perp b})^2 - \frac{\partial_{x_a}(x_a x_b \partial_{x_b})}{(m_a+m_b)^2}\right]$$
$$+ \frac{1}{2}\sum_{a\neq b}\frac{C_F 4\pi\alpha_s}{Q_{ab}^2}\bar{u}_{s'_a}(k'_a)\gamma^\mu u_{s_a}(k_a)\bar{u}_{s'_b}(k'_b)\gamma^\nu u_{s_b}(k_b)g_{\mu\nu}$$

- For the first Fock sector:

$$|qqq\rangle = |n_{q1}, m_{q1}, k_{q1}, \lambda_{q1}\rangle \otimes |n_{q2}, m_{q2}, k_{q2}, \lambda_{q2}\rangle \otimes |n_{q3}, m_{q3}, k_{q3}, \lambda_{q3}\rangle$$

- Transverse : 2D harmonic oscillator basis $\phi_{nm}(\vec{p}_\perp)$;
  Plane wave basis in longitudinal direction.
- The valence wavefunction in momentum space:

$$\Psi^{M_J}_{\{x_i,\vec{p}_{\perp i},\lambda_i\}} = \sum_{n_i,m_i}\left[\psi(\alpha_i)\prod_{i=1}^{3}\phi_{n_i m_i}(\vec{p}_{\perp i})\right]$$

Nucleon Form Factors

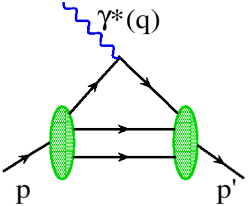

$$G_E(q^2) = F_1(q^2) - \frac{q^2}{4M^2}F_2(q^2),$$

$$G_M(q^2) = F_1(q^2) + F_2(q^2).$$

$$\langle P';\uparrow|\frac{J^+(0)}{2P^+}|P;\uparrow\rangle = F_1(q^2)$$

$$\langle P';\uparrow|\frac{J^+(0)}{2P^+}|P;\downarrow\rangle = -(q^1 - iq^2)\frac{F_2(q^2)}{2M}$$

Drell & Yan (PRL, 70); West (PRL, 70)

$N_{\max} = 10, \ K = 16.5$

Basis truncation :

$$\sum_i (2n_i + |m_i| + 1) \le N_{\max}; \quad K = \sum_i k_i$$

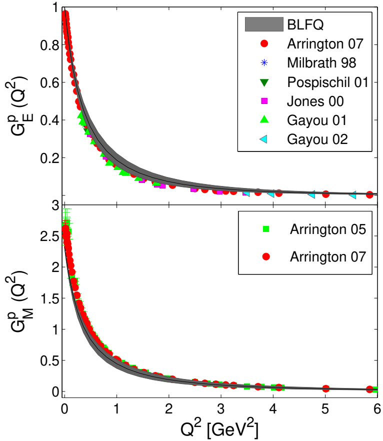

[1] CM, Siqi Xu, *et. al.*, Phys. Rev. D **102**, 016008 (2020)

[2] Xu, CM, Lan, Zhao, Li, and Vary, Phys. Rev. D 104, 094036 (2021)

Ratio of Form Factors

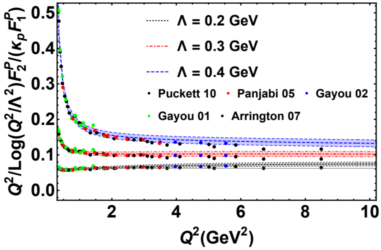

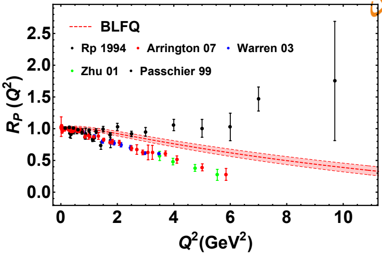

- Consistent with PQCD prediction [1]: $Q^2 F_2^p / F_1^p \sim \log^2[Q^2/\Lambda^2]$
- Only valence quarks contributions
- Missing meson-cloud effects
- $|qqqq\bar{q}\rangle$ has a significant effect on Pauli FF: 30% in proton; 40% in neutron

Sufian *et. al.* PRD 95 (2017)

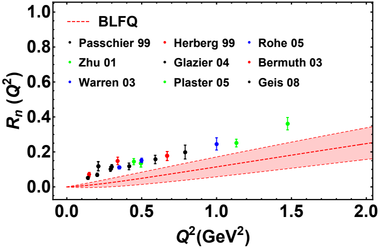

$R \sim G_E/G_M$

[1] Belitsky, Ji, and Yuan, Phys. Rev. Lett. 91, 092003 (2003)

[2] Xu, CM, Lan, Zhao, Li, and Vary, Phys. Rev. D 104, 094036 (2021)

Axial Form Factor

$$\langle N(p)|A^\mu|N(p')\rangle = \bar{u}(p')\left[\gamma^\mu G_A(t) + \frac{(p'-p)^\mu}{2m} G_p(t)\right]\gamma_5 u(p)$$

- Axial vector current: $A^\mu = \bar{q}\gamma^\mu\gamma_5 q$
- Measured by ordinary muon capture (OMC)

$$\mu^-(l) + p(r) \to \nu_\mu(l') + n(r')$$

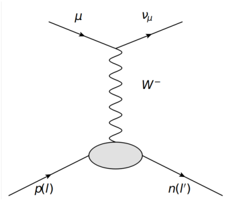

- Provide information on spin distributions

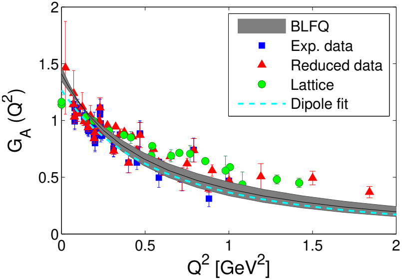

$$G_A(Q^2) = G_u(Q^2) - G_d(Q^2)$$

[1] CM, Siqi Xu *et. al.*, Phys. Rev. D **102**, 016008 (2020)

Parton Distribution Functions

Xu, CM, Lan, Zhao, Li, and Vary, PRD 104, 094036 (2021)

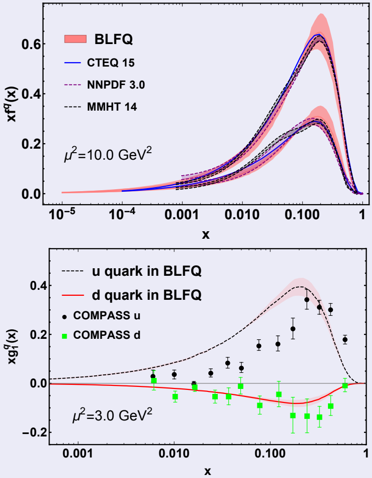

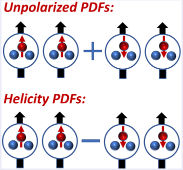

- Unpolarized PDFs $f_1(x)$: longitudinal momentum distribution of unpol. quark in unpol. proton.
- Helicity PDFs $g_1(x)$: longitudinal momentum distribution of the polarized quark
- Results correspond to leading Fock sector only.

[1] NNPDF, EPJC 77, 663 (2017); HMMT, EPJC 75, 204 (2015); CTEQ, PRD 93, 033006 (2016).
[2] COMPASS Collaboration, Phys. Lett. B 693, 227 (2010).

Transversity Distribution

Xu, CM, Lan, Zhao, Li, and Vary, PRD 104, 094036 (2021)

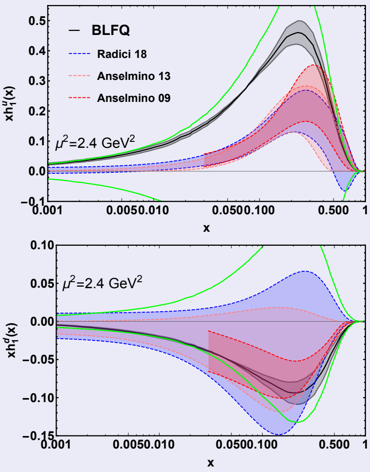

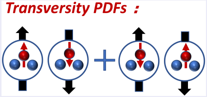

- Transversity PDFs
  describe correlation between the transverse polarization of the nucleon and the transverse polarization of the parton.
- Satisfy Soffer Bound:

$$|h_1(x)| \leq \frac{1}{2}|f_1(x) + g_1(x)|$$

- Results correspond to leading Fock sector only, missing higher Fock sectors.

[1] M. Radici and A. Bacchetta, Phys. Rev. Lett. 120, 192001 (2018).
[2] M. Anselmino, *et. al.*, Phys. Rev. D 87, 094019 (2013).

GPDs for Spin-1/2 Target

$$\frac{P^+}{2\pi}\int dy^- e^{ixP^+y^-}\langle p'|\bar{\psi}_q(-y/2)\gamma^+\psi_q(y/2)|p\rangle\Big|_{y^+=\vec{y}_\perp=0}$$
$$= H^q(x,\xi,t)\,\bar{u}(p')\gamma^+u(p) + E^q(x,\xi,t)\,\bar{u}(p')i\sigma^{+\nu}\frac{\Delta_\nu}{2M_n}u(p)\,,$$

Off-forward matrix elements

In momentum space no probabilistic interpretation

➢GPDs in impact parameter space: $\mathcal{X}(x,b) = \frac{1}{2\pi}\int d^2\Delta e^{-i\Delta^\perp\cdot b^\perp}\mathcal{X}(x,t).$

At t=0, 2nd moment of GPDs: angular momentum

$$J^q = \frac{1}{2}[A^q(0) + B^q(0)]$$

Second moment of GPDs give gravitational FFs

$$\int_0^1 dx\, xH_v^q(x,t) = A^q(t), \quad \int_0^1 dx\, xE_v^q(x,t) = B^q(t)$$

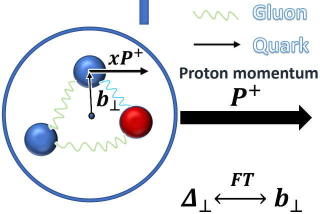

[1] Ji, Phys. Rev. Lett. 78, 610 (1997); Burkardt, Int. J. Mod. Phys. A 18, 173-208 (2003)

Valence Quark Leading Twist GPDs in Proton

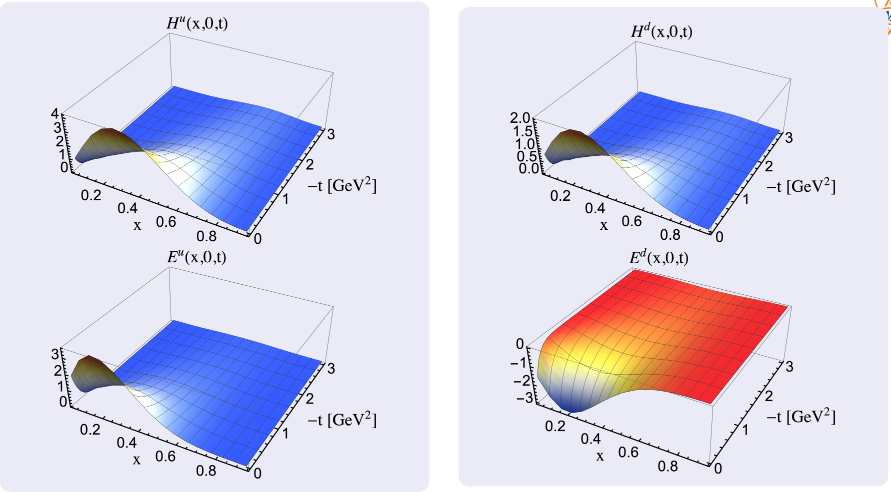

- Qualitative nature consistent with phenomenological models [2]

[1] Y. Liu, S. Xu, CM, X. Zhao, J. P. Vary, arXiv:2202.00985 [hep-ph].
[2] CM, D. Chakrabarti, EPJC 75, 261 (2015); PRD 88, 073006 (2013)

x-Dependent Squared Radius

$$\langle b_\perp^2 \rangle^q(x) = \frac{\int d^2\vec{b}_\perp b_\perp^2 H^q(x, b_\perp)}{\int d^2\vec{b}_\perp H^q(x, b_\perp)},$$

- Transverse squared radius:

$$\langle b_\perp^2 \rangle = \sum_q e_q \int_0^1 \mathrm{d}x f^q(x) \langle b_\perp^2 \rangle^q(x)$$

- BLFQ result: $\langle b_\perp^2 \rangle = 0.40 \pm 0.04$ fm^2
- Experimental data [2]: $\langle b_\perp^2 \rangle_{\text{exp}} = 0.43 \pm 0.01$ fm^2

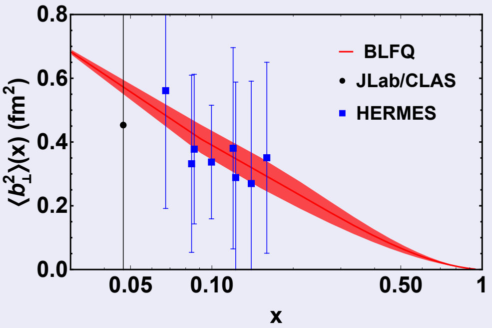

[1] Xu, CM, Lan, Zhao, Li, and Vary, PRD 104, 094036 (2021)
[2] R. Dupre, M. Guidal and M. Vanderhaeghen, PRD 95, 011501 (2017).

Other Observables

- The magnetic moment of the proton and neutron

Quantity	BLFQ	Measurement[a]	Lattice
μ_{p}	2.443 ± 0.027	2.79	2.43(9)
μ_{n}	-1.405 ± 0.026	-1.91	$-1.54(6)$

- The radii of the proton and neutron

Quantity	BLFQ	Measurement	Lattice
$r_{\mathrm{E}}^{\mathrm{p}}$ [fm]	$0.802^{+0.042}_{-0.040}$	0.833 ± 0.010	0.742(13)
$r_{\mathrm{M}}^{\mathrm{p}}$ [fm]	$0.834^{+0.029}_{-0.029}$	0.851 ± 0.026	0.710(26)
$\langle r_{\mathrm{E}}^2 \rangle^{\mathrm{n}}$ [fm^2]	-0.033 ± 0.198	-0.1161 ± 0.0022	$-0.074(16)$
$r_{\mathrm{M}}^{\mathrm{n}}$ [fm]	$0.861^{+0.021}_{-0.019}$	$0.864^{+0.009}_{-0.008}$	0.716(29)

- The axial charge and axial radius

Quantity	BLFQ	Extracted data	Lattice
g_{A}^{u}	1.16 ± 0.04	0.82 ± 0.07	0.830(26)
g_{A}^{d}	-0.248 ± 0.027	-0.45 ± 0.07	$-0.386(16)$
g_{A}^{u-d}	1.41 ± 0.06	1.2723 ± 0.0023	1.237(74)
$\sqrt{\langle r_{\mathrm{A}}^2 \rangle}$ fm	$0.680^{+0.070}_{-0.073}$	0.667 ± 0.12	0.512(34)

[1] Lattice: Alexandrou:2018sim; Yao:2017fvm; Alexandrou:2017ooh

Angular Momentum Distributions

- Spin decomposition

Jaffe-Manohar Decomposition

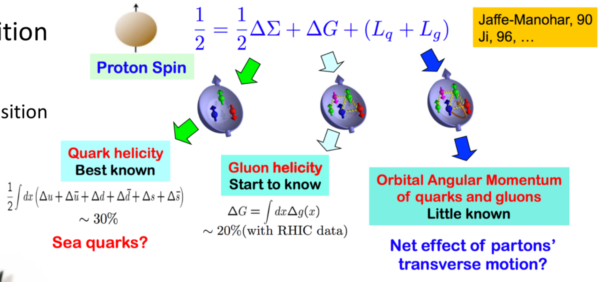

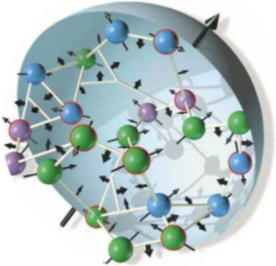

In the quark model $\Delta\Sigma = 1$
The spin decomposition can be measured by polarized DIS

- Ji decomposition:

$$\frac{1}{2} = \frac{1}{2}\Delta\Sigma + L^q_{Ji} + J_g$$

Ji sum rule: $J^{q/g} = \frac{1}{2}\int \mathrm{d}x\, x\, [H^{q/g}(x,0,0) + E^{q/g}(x,0,0)]$

Angular Momentum Distributions in Transverse Plane

- The $b_\perp$ dependent distributions of kinetic OAM and spin in light-front:

$$\langle L^z \rangle (b_\perp) = -\iota\varepsilon^{3jk} \int \frac{\mathrm{d}^2\vec{\Delta}_\perp}{(2\pi)^2}\, e^{-\iota\vec{\Delta}_\perp\cdot\vec{b}_\perp}\, \frac{\partial\langle T^{+k}\rangle}{\partial\Delta_\perp^j}\bigg|_{\mathrm{DY}}$$

$$= \Lambda^z \int \frac{\mathrm{d}^2\vec{\Delta}_\perp}{(2\pi)^2}\, e^{-\iota\vec{\Delta}_\perp\cdot\vec{b}_\perp} \left[L(t) + t\,\frac{\mathrm{d}L(t)}{\mathrm{d}t}\right]$$

$$\langle S^z \rangle (b_\perp) = \frac{1}{2}\,\varepsilon^{3jk} \int \frac{\mathrm{d}^2\vec{\Delta}_\perp}{(2\pi)^2}\, e^{-\iota\vec{\Delta}_\perp\cdot\vec{b}_\perp}\, \langle S^{+jk}\rangle\Big|_{\mathrm{DY}}$$

$$= \frac{\Lambda^z}{2} \int \frac{\mathrm{d}^2\vec{\Delta}_\perp}{(2\pi)^2}\, e^{-\iota\vec{\Delta}_\perp\cdot\vec{b}_\perp}\, G_A(t)$$

where $L(t) == \frac{1}{2}\left(A(t) + B(t) - G_A(t)\right)$

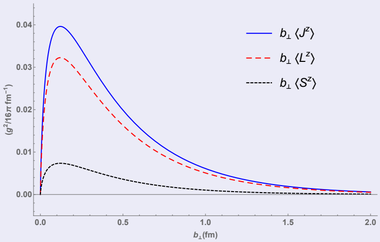

$$\langle J^z \rangle (b_\perp) = \langle L^z \rangle (b_\perp) + \langle S^z \rangle (b_\perp)$$

Cédric Lorcé et al., Phys. Lett. B 776 (2018) 38-47

Flavor contributions: [Liu, Xu, CM, Zhao and Vary, accepted in PRD]

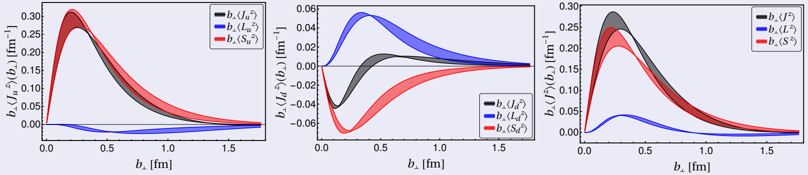

Twist-3 GPDs & OAM

BLFQ calculation:

Stephan Meißner *et al* JHEP08(2009)056

Parameterization:
$$F^{[\gamma^j]}_{\lambda\lambda'} = \frac{M}{2(P^+)^2}\,\bar{u}(p',\lambda')\Big[i\sigma^{+j}\,H_{2T}(x,\xi,t) + \frac{\gamma^+\Delta^j_T - \Delta^+\gamma^j}{2M}\,E_{2T}(x,\xi,t) + \frac{P^+\Delta^j_T - \Delta^+P^j_T}{M^2}\,\tilde{H}_{2T}(x,\xi,t) + \frac{\gamma^+P^j_T - P^+\gamma^j}{M}\,\tilde{E}_{2T}(x,\xi,t)\Big]\,u(p,\lambda)\,,$$

d quark **u quark**

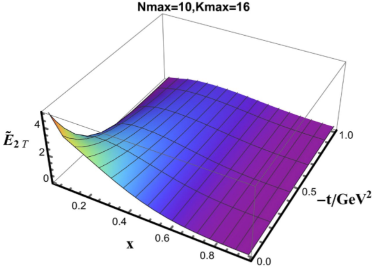

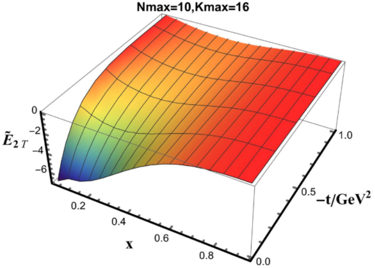

H_{2T}, E_{2T} and $\widetilde{H}_{2T}$ are 0 at zero-skewness($\xi = 0$).

[2] Ziqi Zhang *et. al.*, in preparation

Twist-3 GPDs & OAM

OAM density distribution:

Polyakov et al.

$$\mathcal{F}_{\perp\mu}(x,\xi,\Delta) = \bar{N}(P',S') \times \left\{ (H+E)\,\gamma_\mu^\perp + G_1 \frac{\Delta_\mu^\perp}{2M} + G_2\,\gamma_\mu^\perp + G_3\,\Delta_\mu^\perp \hat{n} + G_4\, i\varepsilon_{\mu\nu}^\perp \Delta_\perp^\nu \hat{n}\gamma_5 \right\} \times N(P,S),$$

Ji's proton's angular momentum sum rule:

$$\frac{1}{2} = J_q + J_g = \frac{1}{2}\Delta\Sigma + L_q + J_g,$$

The contribution of quark OAM can be related to twist-3 and twist-2 GPDs:

$$L^q = -\int dx\, x G_2^q(x,0,0) = -\frac{1}{2}\left[-\int dx\, x\left(H^q(x,0,0) + E^q(x,0,0)\right) + \int dx \widetilde{H}^q(x,0,0)\right],$$

where $G_2^q = -H^q - E^q - \tilde{E}_{2T}^q$.

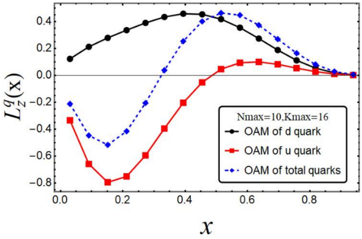

Integrated value: 0.0450337

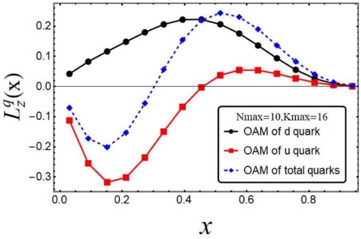

Integrated value: 0.0450337

[1] Courtoy, Goldstein, Gonzalez Hernandez, Liuti and Rajan, Phys. Lett. B **731**, 141-147 (2014)

[2] Ziqi Zhang *et. al.*, in preparation

TMDs of Spin-1/2 Target

Leading Twist TMDs

Nucleon Spin | Quark Spin

		Quark Polarization		
		Un-Polarized (U)	**Longitudinally Polarized (L)**	**Transversely Polarized (T)**
Nucleon Polarization	**U**	f_1 =		$h_1^\perp$ = − Boer-Mulders
	L		g_{1L} = − Helicity	$h_{1L}^\perp$ = −
	T	$f_{1T}^\perp$ = − Sivers	$g_{1T}^\perp$ = −	h_1 = − Transversity $h_{1T}^\perp$ = −

- 6 T-even TMDs and 2 T-odd TMDs.

[1] A. Accardi *et al.*, Eur.Phys.J.A 52 (2016) 9, 268.

Quark TMDs in Proton

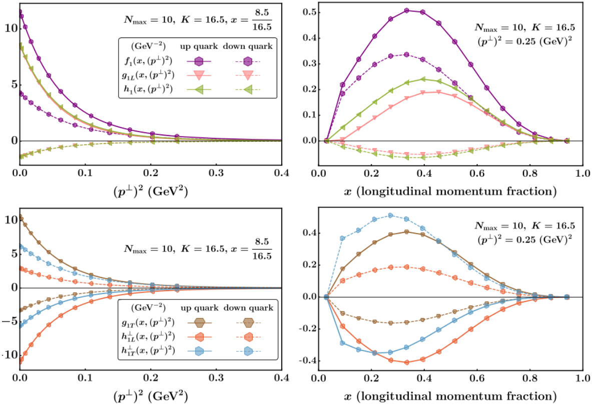

qualitative agreement with other theoretical calculations

[10.1103/PhysRevD.81.074035; 10.1103/PhysRevD.80.014021; 10.1103/PhysRevD.103.014024; 10.1103/PhysRevD.78.074010; 10.1103/PhysRevD.95.074009; 10.1103/PhysRevD.78.034025; 10.1103/PhysRevD.83.094507; 10.1103/PhysRevD.85.094510; 10.1103/PhysRevD.96.094508]

[1] Zhi Hu, Siqi Xu, CM, Xingbo Zhao, J. P. Vary, in preparation

Flavor-Ratios Compared with Lattice QCD

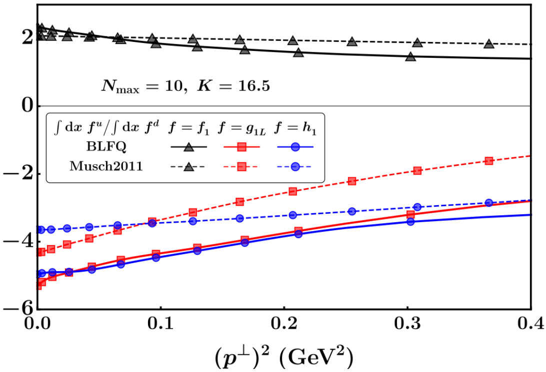

- comparison with lattice results Musch2011 [10.1103/PhysRevD.83.094507]
- ratio cancel possible overall factors and effects from scale evolution
- our d quark distributions extend to higher $(p^\perp)^2 \to$ our flavor ratio decrease faster

[1] Zhi Hu, Siqi Xu, CM, Xingbo Zhao, J. P. Vary, in preparation

x and Flavor Dependence of $\langle(p_\perp^2)\rangle$

$$\langle(p^\perp)^2\rangle_f^q(x) = \frac{\int d^2p^\perp\,(p^\perp)^2 f^q_{\rm BLFQ}(x,(p^\perp)^2)}{\int d^2p^\perp\, f^q_{\rm BLFQ}(x,(p^\perp)^2)}$$

- strong x and flavor dependence of $\langle(p^\perp)^2\rangle$
- don't support $x - p^\perp$ factorization
- universal structure with a peak

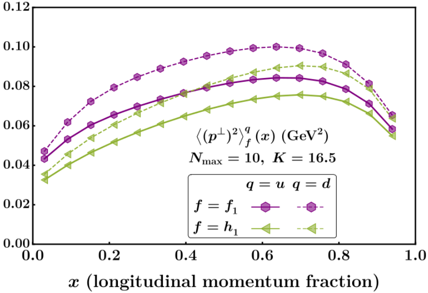

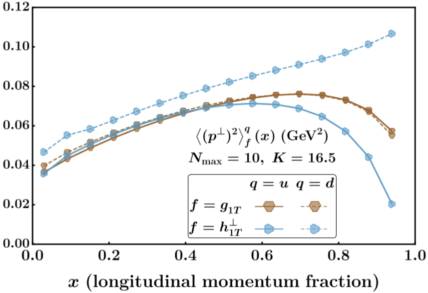

[1] Zhi Hu, Siqi Xu, CM, Xingbo Zhao, J. P. Vary, in preparation

Comparison with Gaussian Ansatz

$$f^q_{\text{Gaus.}}(x, (p^\perp)^2) = f^q_{\text{BLFQ}}(x) \frac{\exp\left(-\frac{(p^\perp)^2}{\langle (p^\perp)^2 \rangle^q_f(x)}\right)}{\pi \langle (p^\perp)^2 \rangle^q_f(x)}$$

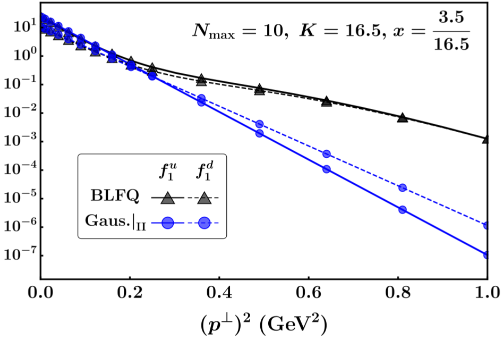

- **small** $(p^\perp)^2$ **region**: Gaussian-type distributions with x-dependent Gaussian width
- **large** $(p^\perp)^2$ **region**: BLFQ results decrease slower than Gaussian-type distributions
- **perturbative results**: $f_1 \sim 1/p^2$ in the large $(p^\perp)^2$ region [10.1088/1126-6708/2008/08/023]

[1] Zhi Hu, Siqi Xu, CM, Xingbo Zhao, J. P. Vary, in preparation

Effective Hamiltonian with One Dynamical Gluon

$$| \text{Baryon}\rangle = a\,| qqq\rangle + b\,| qqqg\rangle + c\,| qqqq\bar{q}\rangle + \ldots$$

kinetic energy

transverse confining potential [2]

$$H_{\text{eff}} = \sum_a \frac{\vec{p}^{\,2}_{\perp a} + m_a^2}{x_a} + \frac{1}{2}\sum_{a\neq b}\kappa^4\left[x_a x_b(\vec{r}_{\perp a} - \vec{r}_{\perp b})^2\right]$$

$$-\frac{1}{2}\sum_{a\neq b}\kappa^4\left[\frac{\partial_{x_a}(x_a x_b \partial_{x_b})}{(m_a+m_b)^2}\right] + H_{\text{vertex}} + H_{\text{inst}}$$

longitudinal confining potential [3]

QCD interactions [4]

[1] S. Xu, CM, X. Zhao, Y. Li, J. P. Vary, work in progress.
[2] Brodsky, Teramond, Dosch and Erlich, Phys. Rep. 584, 1 (2015).
[3] Li, Maris, Zhao and Vary, Phys. Lett. B (2016).
[4] Brodsky, Pauli, and Pinsky, Phys. Rep. 301, 299 (1998).

QCD Interactions

$$|P_{baryon}\rangle = \psi_1|qqq\rangle + \psi_2|qqqg\rangle$$

$$H_{Interact} = H_{Vertex} + H_{inst} = g\bar{\psi}\,\gamma^\mu T^a\,\psi\,A^a_\mu + \frac{g^2 C_F}{2}\,j^+\,\frac{1}{(i\partial^+)^2}\,j^+$$

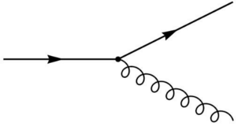

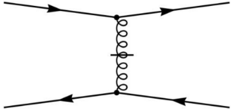

$$N_{\max} = 9, K = 16.5$$

Higher Fock Sector effect

Remove Soft Gluon effect

m_u	m_d	κ	m_g	m_{int}	b_{inst}	b	g
0.30 GeV	0.25 GeV	0.54 GeV	0.50 GeV	1.80 GeV	3.00 GeV	0.70 GeV	2.40

Different Mass Asymmetry of u and d

UV Cutoff In Instantaneous term

Unpolarized PDFs

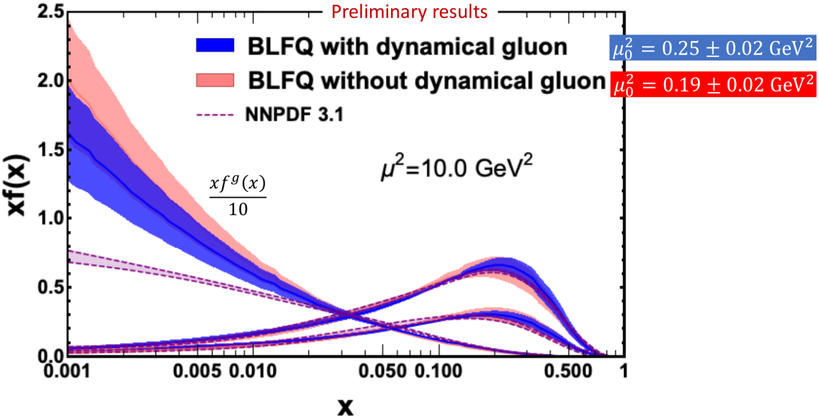

- Within $|qqq\rangle$, gluon is generated dynamically from the DGLAP evolution.
- Including dynamical gluon, the gluon distribution is closer to the global fit.

Unpolarized PDFs

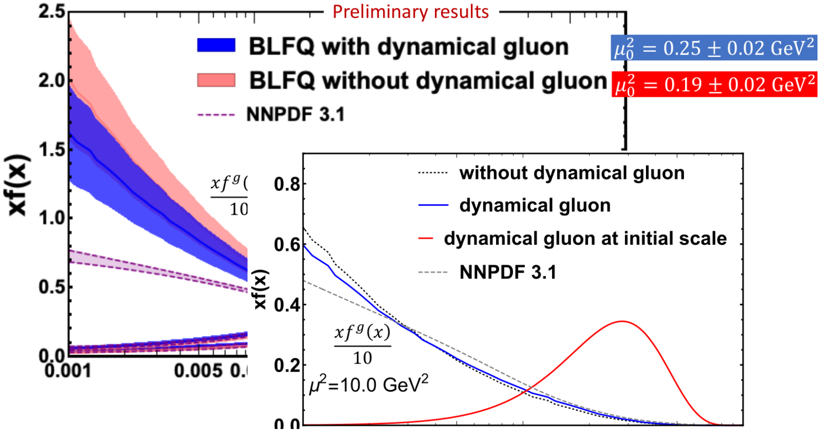

- Within $|qqq\rangle$, gluon is generated dynamically from the QCD evolution.
- Including dynamical gluon, the gluon distribution is closer to the global fit.

Helicity PDFs

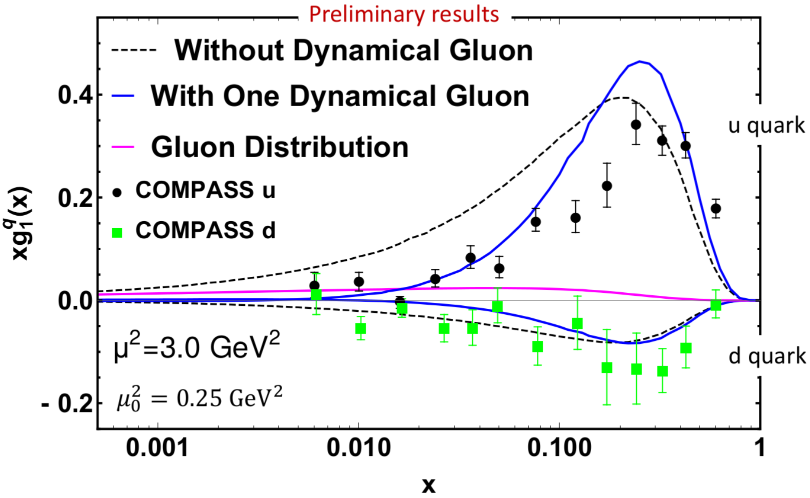

- Including dynamical gluon, the distributions improve at small x and $x > 0.5$.

Gluon GPDs

Meissner, Metz and Goeke, PRD 76, 034002 (2007)

$$F^g(x,\Delta;\lambda,\lambda') = \frac{1}{2P^+}\,\bar{u}(p',\lambda')\left(\gamma^+\,H^g(x,\xi,t) + \frac{i\sigma^{+\mu}\Delta_\mu}{2M}\,E^g(x,\xi,t)\right)u(p,\lambda)\,,$$

$$\tilde{F}^g(x,\Delta;\lambda,\lambda') = \frac{1}{2P^+}\,\bar{u}(p',\lambda')\left(\gamma^+\gamma_5\,\tilde{H}^g(x,\xi,t) + \frac{\Delta^+\gamma_5}{2M}\,\tilde{E}^g(x,\xi,t)\right)u(p,\lambda)\,.$$

Preliminary

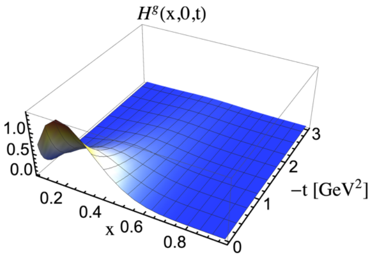

[1] S. Xu, CM, X. Zhao, Y. Li, J. P. Vary, work in progress.

GTMDs & OAM

Generalized Transverse-Momentum Parton Distribution functions

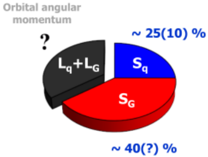

$$W_{\lambda\lambda'}^{[\gamma^+]}(P,x,\vec{k}_\perp,\Delta)=\frac{1}{2}\int\frac{dz^- d^2\vec{z}_\perp}{(2\pi)^3}e^{ik\cdot z}\left\langle p',\lambda'\left|\overline{\psi}\left(-\frac{1}{2}z\right)\gamma^+\psi\left(\frac{1}{2}z\right)\right|p,\lambda\right\rangle$$

$$W_{\lambda\lambda'}^{[\delta^{ij}]}(P,x,\vec{k}_\perp,\Delta)=\frac{1}{xP^+}\int\frac{dz^- d^2\vec{z}_\perp}{(2\pi)^3}e^{ik\cdot z}\left\langle p',\lambda'\left|G^{+i}\left(-\frac{1}{2}z\right)G^{+i}\left(\frac{1}{2}z\right)\right|p,\lambda\right\rangle$$

Parameterization:

$$W_{\lambda\lambda'}^{[\gamma^+]}(P,x,\vec{k}_\perp,\Delta)=W_{\lambda\lambda'}^{[\delta^{ij}]}(P,x,\vec{k}_\perp,\Delta)$$
$$=\frac{1}{2M}\overline{u}(p',\lambda')\left[F_{1,1}+\frac{i\sigma^{j+}}{p^+}(k_\perp^j F_{1,2}+\Delta_\perp^j F_{1,3})+i\frac{\sigma^{ij}k_\perp^i\Delta_\perp^j}{M^2}F_{1,4}\right]u(p,\lambda)$$

$F_{1,4}$ is related to the orbital angular momentum

$$L_{q,g}(x)=-\int d^2k_\perp\frac{k_\perp^2}{M^2}F_{1,4}(x,k_\perp,\Delta_\perp=0)$$

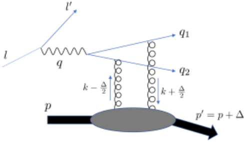

[1] S. Bhattacharya, R. Boussarie and Y. Hatta, arXiv-hep:2201.08709 (2022)

GTMDs

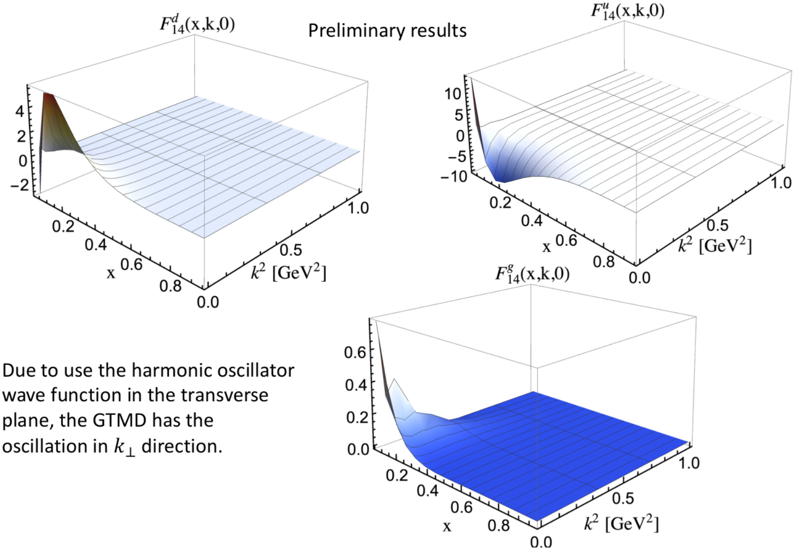

Due to use the harmonic oscillator wave function in the transverse plane, the GTMD has the oscillation in $k_\perp$ direction.

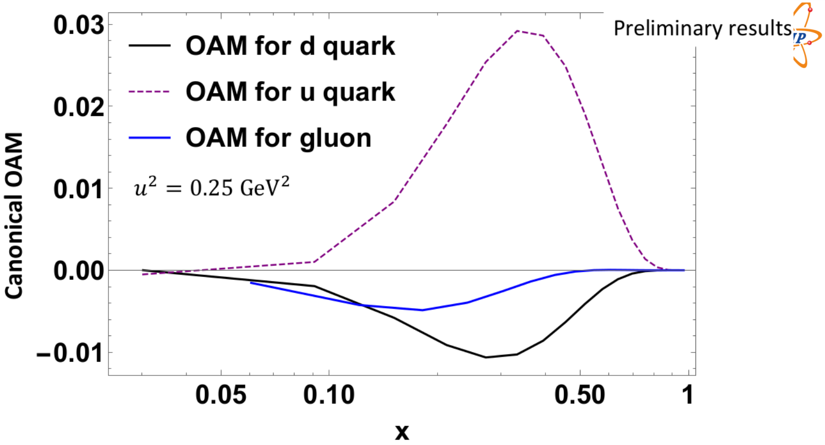

Canonical: $\ell_g = -0.007$ $\ell_u = 0.033$ $\ell_d = -0.013$

Kinetic : $\frac{1}{2}\Delta\Sigma = 0.36$ $L_q = 0.084$ $J_g = 0.0557$

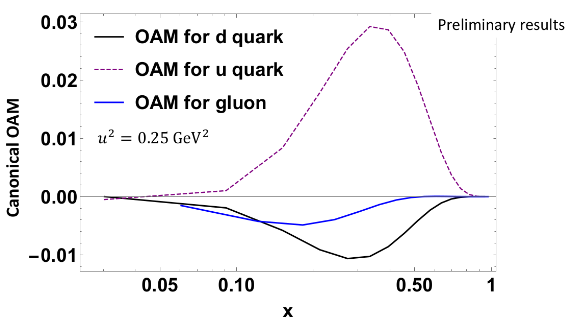

(a) Kinetic

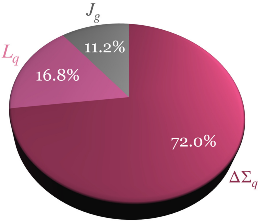

(b) Canonical

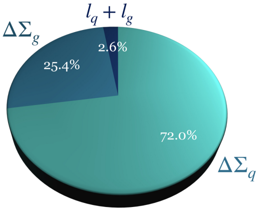

Conclusions

- Light-front Hamiltonian approach: Mass spectra ⇔ Structure
- $|q\bar{q}\rangle$ & $|q\bar{q}g\rangle$ for mesons, $|qqq\rangle$ & $|qqqg\rangle$ for nucleon.
- LF Hamiltonian ⇒ Wavefunctions ⇒ Observables.
- Provides good description of exp. data/global fits for various observables.
- TMDs are consistent with Gaussian-type distributions in the small $p_\perp^2$; and with perturbative calculations in the large $p_\perp^2$.
- Preliminary results on gluon distributions of mesons and nucleon.
- With dynamical gluons, the quark spin contribution (70%) is reduced and the gluon spin plays a substantial role in understanding the nucleon spin.
- *This is not a complete picture ... long way to go*.

Enormous amount of possibilities with future EICs ... ... Thank You

$\pi \to \gamma^* \gamma^*$ Transition Form Factor

$$F_{\pi\gamma^*}(Q_1^2, Q_2^2) = \frac{\sqrt{2}}{3} f_\pi \int_0^1 \mathrm{d}x\, T_{\mathrm{H}}^{\gamma^*\gamma^* \to \pi^0}(x, Q_1^2, Q_2^2)\, \phi(x, \bar{Q})$$

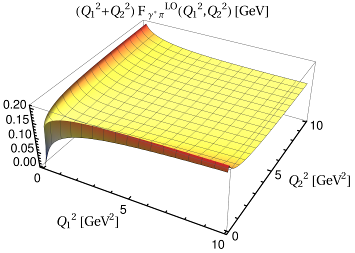

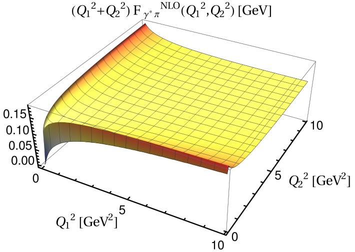

- $F_{\pi\gamma^*}(Q_1^2, Q_2^2) \sim 1/(Q_1^2 + Q_2^2)$ when $(Q_1^2, Q_2^2) \to \infty$.
- Consistent with pQCD prediction.
- Qualitative behavior $\to$ consistent with the LFQM results.
  Choi, Ryu and Ji, PRD 99, 076012 (2019)
- Singly virtual TFF $\to$ by setting one of the momentum transfers to zero.

[1] CM, Nair, Jia, Zhao and Vary, Phys. Rev. D 104, 094034 (2021)

Generalized Parton Distributions (GPDs) : Spin-0 Meson

Two independent GPDs at leading twist

$$H^{\mathcal{P}}(x,\zeta,t) = \int \frac{dz^-}{4\pi} e^{ixP^+z^-} \langle \mathcal{P}(P')|\bar{\Psi}_q(0)\gamma^+\Psi_q(z)|\mathcal{P}(P)\rangle|_{z^+=0}^{\mathbf{z}^\perp=0}$$

$$\frac{i\epsilon_{ij}^\perp q_i^\perp}{2M_{\mathcal{P}}} E_T^{\mathcal{P}}(x,\zeta,t) = \int \frac{dz^-}{4\pi} e^{ixP^+z^-} \langle \mathcal{P}(P')|\bar{\Psi}_q(0)i\sigma^{j+}\gamma_5\Psi(z)_q|\mathcal{P}(P)\rangle|_{z^+=0}^{\mathbf{z}^\perp=0}$$

- $H \Rightarrow$ chirally even unpolarized quark GPD
- $E_T \Rightarrow$ chirally odd; transversely polarized quark GPD
- $P(P')$ denotes the meson momentum of initial (final) state of the meson ($\mathcal{P}$).
- We choose $A^+ = 0$ and the kinematical region: $0 < x < 1$ at zero skewnes ($\zeta = 0$).

[1] *M. Diehl, Phys. Rept. 388, 41 (2003).*

Results: Pion GPDs

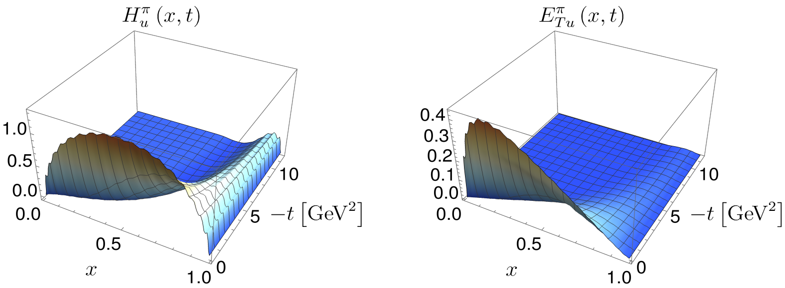

- $H_u^\pi(x,0) \Rightarrow$ symmetric with peak at $x = 0.5$
- $E_{Tu}^\pi(x,0) \Rightarrow$ asymmetric with peak below $x = 0.5$
- peak in the GPDs shift towards higher values of x
- oscillations are numerical artifacts due to longitudinal cutoff $L_{\max}$

[1] Adhikari, CM, Nair, Xu, Jia, Zhao and Vary, [arXiv:2106.04954] accepted by Phys. Rev. D

GPDs → Transverse Densities

- Moments of GPDs:

$$\int_0^1 dx\, x^{n-1} H^{\pi}(x, b_\perp^2) = A^{\pi}_{n0}(b_\perp^2)\,,$$
$$\int_0^1 dx\, x^{n-1} E^{\pi}_T(x, b_\perp^2) = B^{\pi}_{Tn0}(b_\perp^2)\,.$$

- Define density

$$\rho^n(b_\perp, s_\perp) = \frac{1}{2}\Big[\, A^{\pi}_{n0}(b_\perp^2) - \frac{s_\perp^i\, \epsilon^{ij}\, b_\perp^j}{m_\pi}\, B^{\pi\prime}_{Tn0}(b_\perp^2)\Big]\,,$$

- Reasonable agreement with Lattice QCD

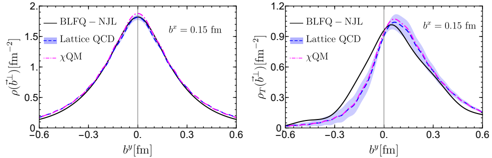

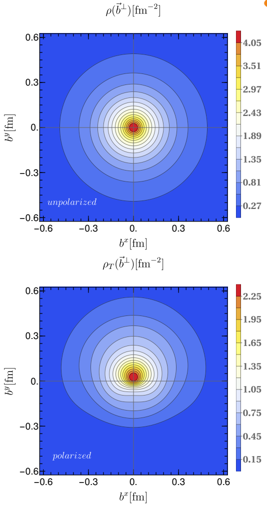

[1] Adhikari, CM, Nair, Xu, Jia, Zhao and Vary, Phys.Rev.D 104, 114019 (2021)

Heavy Meson Mass Spectrum

$$|\text{meson}\rangle = a|Q\overline{Q}\rangle + b|Q\overline{Q}g\rangle + \dots$$

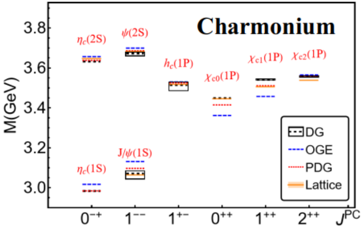

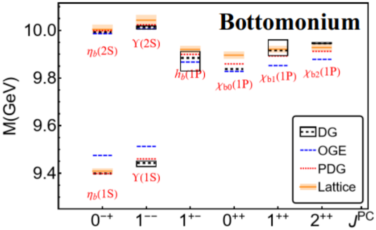

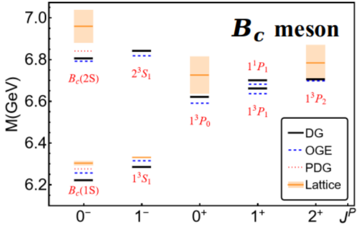

$N_{\max} = 12, K_{\max} = 17$

	$Q\bar{Q}$	m_c (GeV)	m_b (GeV)	$\alpha/\alpha(0)$	$b=\kappa_T=\kappa_L$ (GeV)	m_{fc} (GeV)	m_{fb} (GeV)	m_g (GeV)	b_{inst} (GeV)
OGE	$c\bar{c}$	1.603	...	0.6	0.98	...	...	0.02	...
DG		1.54	...	0.3	1.229	5.04	...	0.5	3.99
OGE	$b\bar{b}$	...	4.902	0.6	1.389	...	...	0.02	...
DG		...	4.78	0.23	1.835	...	13.2	0.5	7.35
OGE	$b\bar{c}$	1.603	4.902	0.6	1.196	...	...	0.02	...
DG		1.54	4.78	0.266	1.562	5.04	13.2	0.5	5.91

OGE ($c\bar{c}$ and $b\bar{b}$) : [Yang Li, et al, 2017]
OGE ($b\bar{c}$) : [Shuo Tang, et al, 2018]

[1] J. Wu *et. al.*, in preparation

Wavefunction in Leading Fock Sector

$$\Psi^{\mathcal{N},M_J}_{\{x_i,\vec{p}^2_{\perp i},\lambda_i\}} = \sum_{\{n_i m_i\}} \psi^{\mathcal{N}}(\{\bar{\alpha}_i\}) \prod_{i=1}^{\mathcal{N}} \phi_{n_i m_i}(\vec{p}_{\perp i}, b)$$

$$|\text{meson}\rangle = a|Q\bar{Q}\rangle + b|Q\bar{Q}g\rangle + \cdots$$

$\downarrow\uparrow - \uparrow\downarrow$ dominant in $|Q\bar{Q}\rangle$

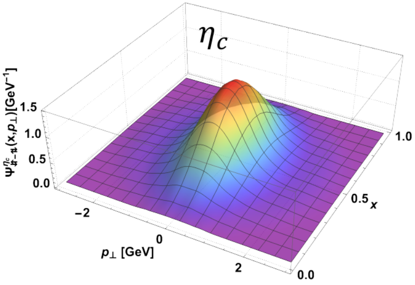

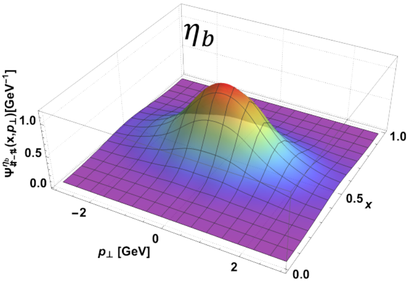

- η_b narrower than η_c at x direction
- η_b wider than η_c at x direction

[1] J. Wu *et. al.*, in preparation

Heavy Meson Electromagnetic Form Factors

[Brodsky & de Teramond, PRD 77:056007 (2008)]

$$|\text{meson}\rangle = a|Q\bar{Q}\rangle + b|Q\bar{Q}g\rangle + \cdots$$

$$\langle\Psi(p')|J^{+}_{EM}(0)|\Psi(p)\rangle = (\mathrm{p}+\mathrm{p}')^{+}\,\mathrm{F}(\mathrm{Q}^2)$$

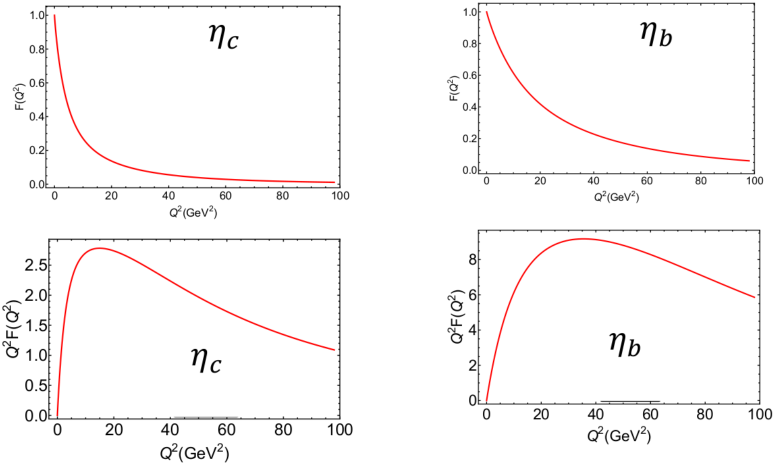

[1] J. Wu *et. al.*, in preparation

Heavy Meson PDAs

$$|\text{meson}\rangle = a|Q\bar{Q}\rangle + b|Q\bar{Q}g\rangle + \cdots$$

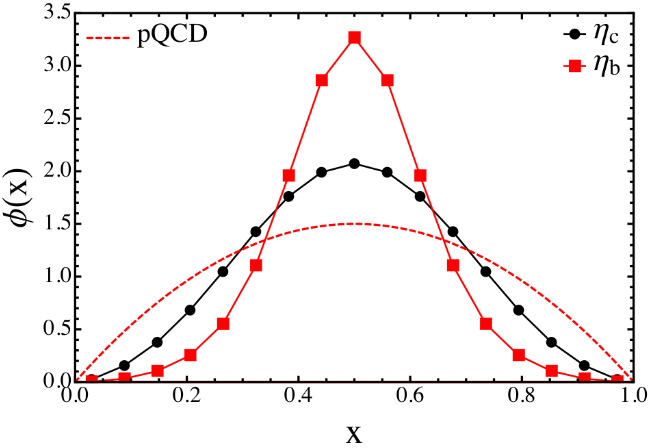

η_b narrower than η_c

Preliminary

[1] J. Wu et. al., in preparation

Heavy Meson GPDs

[M. Diehl, Phys. Rep. 388 (2003) 41-277]

$$|\text{meson}\rangle = a|Q\overline{Q}\rangle + b|Q\overline{Q}g\rangle + \ldots$$

$$H^q_M(x,\xi=0,t) = \frac{1}{2}\int \frac{dz^-}{2\pi} e^{ixP^+z^-} \left\langle M, P+\frac{\Delta}{2} \middle| \bar{q}\left(-\frac{z}{2}\right)\gamma^+ q\left(\frac{z}{2}\right) \middle| M, P-\frac{\Delta}{2} \right\rangle_{\substack{z^+=0\\ z_\perp=0}}$$

$$H^g_M(x,\xi=0,t) = \frac{1}{P^+}\int \frac{dz^-}{2\pi} e^{ixP^+z^-} \left\langle M, P+\frac{\Delta}{2} \middle| G^{+\mu}\left(-\frac{z}{2}\right) G^+_\mu\left(\frac{z}{2}\right) \middle| M, P-\frac{\Delta}{2} \right\rangle_{\substack{z^+=0\\ z_\perp=0}}$$

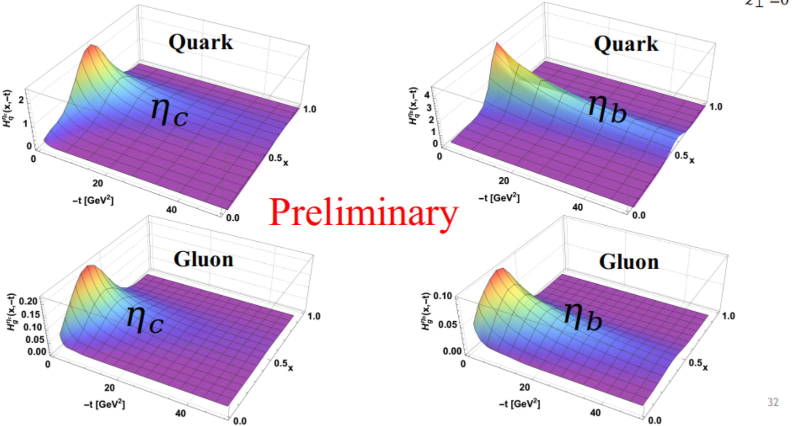

Helicity Asymmetry

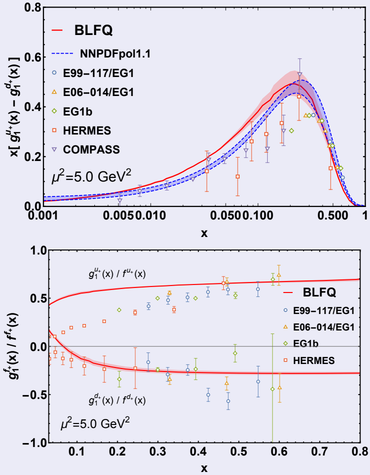

- $q^+(x) = q(x) + \bar{q}(x)$
- The helicity asymmetry: observable for investigating the spin structure of the proton in experiments.
- Overestimated at small-x region.
- Gluon at initial scale is needed within BLFQ.

[1] Xu, CM, Lan, Zhao, Li, and Vary, Phys. Rev. D 104, 094036 (2021)

QCD Interactions

$$|P_{baryon}\rangle = \psi_1|qqq\rangle + \psi_2|qqqg\rangle$$

$$H_{Interact} = H_{Vertex} + H_{inst} = g\bar{\psi}\,\gamma^\mu T^a\,\psi\,A^a_\mu + \frac{g^2 C_F}{2}\,j^+\frac{1}{(i\partial^+)^2}j^+$$

$$N_{\max} = 9, K = 16.5$$

m_u	m_d	κ	m_g	m_{int}	b_{inst}	b	g
0.30 GeV	0.25 GeV	0.54 GeV	0.50 GeV	1.80 GeV	3.00 GeV	0.70 GeV	2.40

- κ → Higher Fock Sector effect
- m_g → Remove Soft Gluon effect
- m_u, m_d → Different Mass Asymmetry of u and d
- b_{inst} → UV Cutoff In Instantaneous term

Tensor Charge

- The first moment of transversity PDF :

$$g_T^q = \int dx\ h_1^q(x, \mu^2)$$

- The second moment of transversity PDF :

$$< x >_T^{u-d} = \int dx\ x\left(h_1^u(x,\mu^2) - h_1^d(x,\mu^2)\right)$$

$g_T^u = 0.55,\ g_T^d = -0.29$ **Dynamical gluon**

$g_T^u = 0.94,\ g_T^d = -0.20$ **No Dynamical gluon**

$g_T^u = 0.39^{+0.18}_{-0.12},\ g_T^d = -0.25^{+0.30}_{-0.10}$ **Extracted data**

Quantity	BLFQ	Extracted data	Lattice
g_T^u	$0.94^{+0.06}_{-0.15}$	$0.39^{+0.18}_{-0.12}$	$0.784(28)$
g_T^d	$-0.20^{+0.02}_{-0.04}$	$-0.25^{+0.30}_{-0.10}$	$-0.204(11)$
$< x >_T^{u-d}$	$0.229^{+0.019}_{-0.048}$	—	$0.203(24)$

Axial Form Factor

- Provide information on spin-isospin distributions

$$\langle N(p')|A^a_\mu|N(p)\rangle = \bar{u}(p')\left[\gamma_\mu G_A(t) + \frac{(p'-p)_\mu}{2m} G_P(t)\right]\gamma_5 \frac{\tau^a}{2} u(p) \qquad A^a_\mu = \bar{q}\gamma_\mu\gamma_5 T^a q$$

Including the dynamic gluon, the u quark's contribution is suppressed and closer to the experimental data results.

$\Delta\Sigma_q \approx 0.7$ $\Delta\Sigma_u \approx 0.86$ $\Delta\Sigma_d \approx 0.16$ $\Delta G \approx 0.13 < 0.2$ (COMPASS)

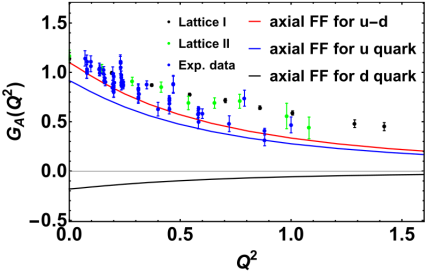

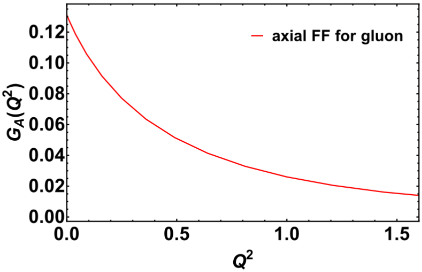

Unpolarized GPDs without dynamical gluon

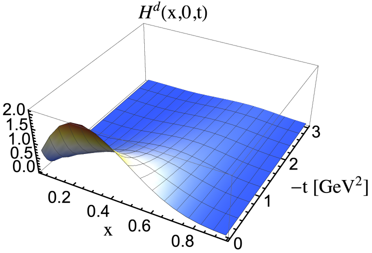

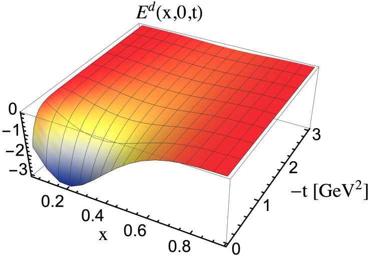

Unpolarized GPDs with dynamical gluon

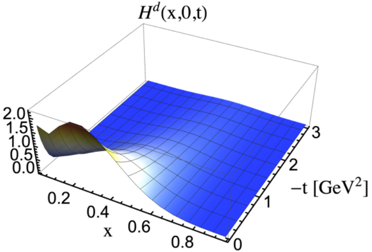

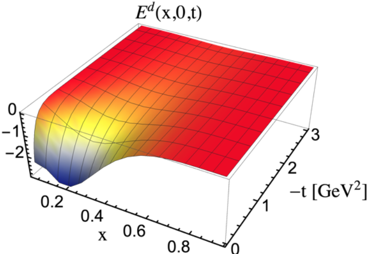

Helicity GPDs without dynamical gluon

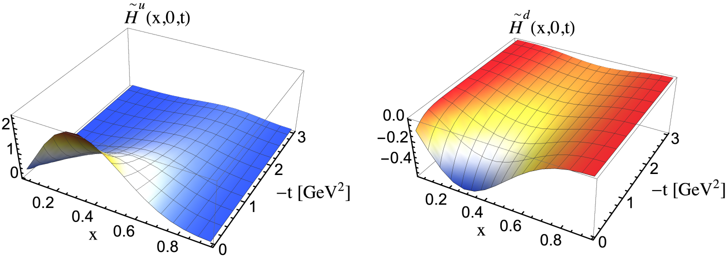

Helicity GPDs with dynamical gluon

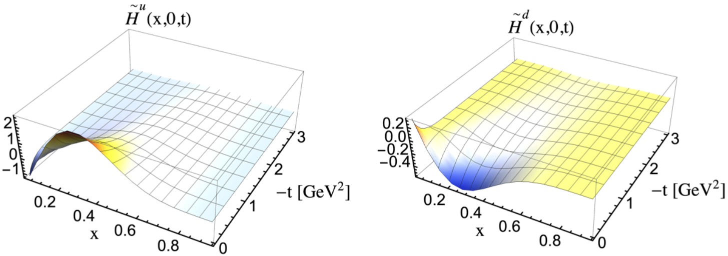

- OAM densities:

$$L^{\text{naive}}(b_\perp) = \tilde{J}(b_\perp) - S(b_\perp)$$

$$L^{\text{PG}}(b_\perp) = \rho_J^{\text{PG}} - S(b_\perp) \qquad [\text{Polyakov} - \text{Goeke(PG)}]$$

$$L^{\text{IMF}}(b_\perp) = \rho_J^{\text{IMF}} - S(b_\perp) \qquad [\text{Infinite Momentum Frame(IMF)}]$$

where $\tilde{J}, \rho_J^{\text{PG}}$ and ρ_J^{IMF} are TAM densities.

$$\rho_J^{\text{PG}}(b_\perp) = \frac{1}{3}\tilde{J}(b_\perp) - \frac{1}{3} b_\perp \frac{d}{db_\perp}\tilde{J}(b_\perp) \quad ; \quad \rho_J^{\text{IMF}}(b_\perp) = \mp\frac{1}{2} b_\perp \frac{d}{db_\perp}\tilde{J}(b_\perp)$$

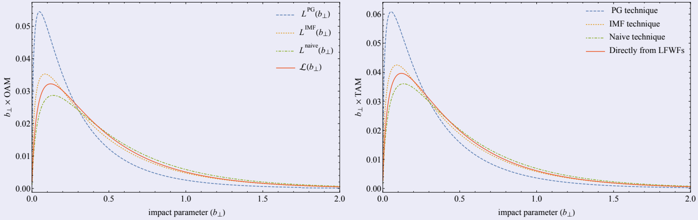

Lekha Adhikari and Matthias Burkardt, et al. Phys. Rev. D 94 (2016) 11, 114021

- OAM distributions from different techniques do not agree with each other.

Fourier Transformation of GPDs ⇒ IPD GPDs

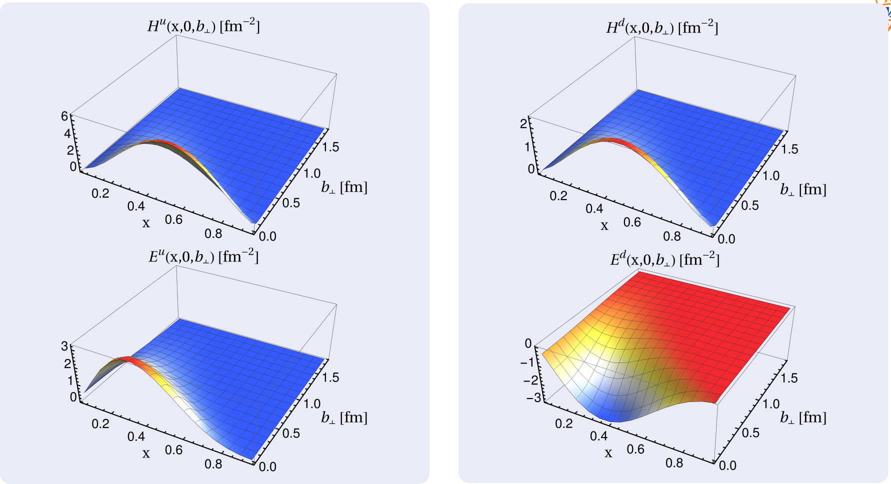

- Qualitative nature consistent with phenomenological models [2]

[1] Y. Liu, S. Xu, CM, X. Zhao, J. P. Vary, arXiv:2202.00985 [hep-ph].
[2] CM, D. Chakrabarti, EPJC 75, 261 (2015); PRD 88, 073006 (2013)

Angular momentum operators

- Generalized angular momentum tensor [1]:

$$J^{\mu\alpha\beta}(y) = L^{\mu\alpha\beta}(y) + S^{\mu\alpha\beta}(y)$$

$L^{\mu\alpha\beta}$: OAM operator; $S^{\mu\alpha\beta}$: spin operator

$$L^{\mu\alpha\beta}(y) = y^\alpha T^{\mu\beta}(y) - y^\beta T^{\mu\alpha}(y)$$

$T^{\mu\nu}$: Energy–Momentum Tensor (EMT) density associated with the system; neither gauge invariant nor symmetric.

1. The Belinfante-improved tensors: conserved and gauge invariant

$$T^{\mu\nu}_{\text{Bel}}(y) = T^{\mu\nu}(y) + \partial_\lambda G^{\lambda\mu\nu}(y)$$

$$J^{\mu\alpha\beta}_{\text{Bel}}(y) = J^{\mu\alpha\beta}(y) + \partial_\lambda \left(y^\alpha G^{\lambda\mu\beta}(y) - y^\beta G^{\lambda\mu\alpha}(y) \right)$$

where $G^{\lambda\mu\nu}$: the superpotential

$$G^{\lambda\mu\nu}(y) = \frac{1}{2}\left(S^{\lambda\mu\nu}(y) + S^{\mu\nu\lambda}(y) + S^{\nu\mu\lambda}(y) \right) = -G^{\mu\lambda\nu}(y)$$

- The total angular momentum:
  $J^{\mu\alpha\beta}_{\text{Bel}}(y) = y^\alpha T^{\mu\beta}_{\text{Bel}} - y^\beta T^{\mu\alpha}_{\text{Bel}}$; $T^{\mu\nu}$: symmetric

[1] C. Lorcé, L. Mantovani and B. Pasquini, Phys. Lett. B 776, 38 (2018).

2 Kinetic tensors

- Ji proposed the kinetic EMT in the context of QCD:

$$T^{\mu\nu}_{\text{kin}}(y) = T^{\mu\nu}_{\text{kin,q}}(y) + T^{\mu\nu}_{\text{kin,g}}(y)$$

  $T^{\mu\nu}_{\text{kin,q}}(y), T^{\mu\nu}_{\text{kin,g}}(y)$ are gauge invariant contributions.

- The kinetic generalized angular momentum tensor:

$$J^{\mu\alpha\beta}_{\text{kin}}(y) = L^{\mu\alpha\beta}_{\text{kin,q}}(y) + S^{\mu\alpha\beta}_{q}(y) + J^{\mu\alpha\beta}_{\text{kin,g}}(y)$$

  with $L^{\mu\alpha\beta}_{\text{kin,q}}(y) = y^{\alpha} T^{\mu\beta}_{\text{kin,q}}(y) - y^{\beta} T^{\mu\alpha}_{\text{kin,q}}(y)$

$$S^{\mu\alpha\beta}_{q}(y) = \tfrac{1}{2}\varepsilon^{\mu\alpha\beta\lambda}\bar{\psi}(y)\gamma_{\lambda}\gamma_5\psi(y)$$

$$J^{\mu\alpha\beta}_{\text{kin,g}}(y) = y^{\alpha} T^{\mu\beta}_{\text{kin,g}}(y) - y^{\beta} T^{\mu\alpha}_{\text{kin,g}}(y)$$

- The gluon total AM can not be divided into orbital and spin contributions; it is local and gauge invariant.

- Relation between Belinfante-improved tensors and kinetic tensors:

$$T^{\mu\nu}_{\text{kin,q}}(y) = T^{\mu\nu}_{\text{Bel,q}}(y) - \frac{1}{2}\partial_{\lambda} S^{\lambda\mu\nu}_{q}(y) \quad ; \quad T^{\mu\nu}_{\text{kin,g}}(y) = T^{\mu\nu}_{\text{Bel,g}}$$

$$L^{\mu\alpha\beta}_{\text{kin,q}}(y) + S^{\mu\alpha\beta}_{q}(y) = J^{\mu\alpha\beta}_{\text{Bel,q}}(y) - \frac{1}{2}\partial_{\lambda}\left(y^{\alpha} S^{\lambda\mu\beta}_{q}(y) - y^{\beta} S^{\lambda\mu\alpha}_{q}(y)\right) ; J^{\mu\alpha\beta}_{\text{kin,g}}(y) = J^{\mu\alpha\beta}_{\text{Bel,g}}(y)$$

Parameterization of EMT

- For spin-1/2 target, the matrix elements of the general local asymmetric $T^{\mu\nu}$ are parametrized as

$$\langle P',\Lambda'|\, T^{\mu\nu}(0)\,|P,\Lambda\rangle = \bar{u}(P',\Lambda')\left(\frac{\bar{P}^{\mu}\bar{P}^{\nu}}{M}A(t) + \frac{\bar{P}^{\mu}\iota\sigma^{\nu\lambda}\Delta_{\lambda}}{4M}(A+B+D)(t)\right.$$
$$\left. + \frac{\Delta^{\mu}\Delta^{\nu} - g^{\mu\nu}\Delta^{2}}{M}C(t) + Mg^{\mu\nu}\bar{C}(t) + \frac{\bar{P}^{\nu}\iota\sigma^{\mu\lambda}\Delta_{\lambda}}{4M}(A+B-D)(t)\right)u(P,\Lambda)$$

- The matrix elements of quark spin operator $S_q^{\mu\alpha\beta}(0)$ are parametrized as:

$$\langle P',\Lambda'|\, S_q^{\mu\alpha\beta}(0)\,|P,\Lambda\rangle = \frac{1}{2}\varepsilon^{\mu\alpha\beta\lambda}\bar{u}(P',\Lambda')\left(\gamma_{\lambda}\gamma_{5}G_A^q(t) + \frac{\Delta_{\lambda}\gamma_{5}}{2M}G_P^q(t)\right)u(P,\lambda)$$

$G_A^q(t)$: axial-vector form factor
$G_P^q(t)$: induced pseudoscalar form factor

- $D_q(t) = -G_A^q(t) \quad ; \quad t = -\Delta_{\perp}^2.$

- Experimentally, axial form factor is accessible through quasi-elastic neutrino scattering and pion electroproduction processes.

[1] Cédric Lorcé et al., Phys. Lett. B 776 (2018) 38-47

- The Belinfante-improved TAM:

$$\langle J^z_{\text{Bel}}\rangle(b_\perp) = -\iota\varepsilon^{3jk}\int \frac{\mathrm{d}^2\vec{\Delta}_\perp}{(2\pi)^2}\, e^{-\iota\vec{\Delta}_\perp\cdot\vec{b}_\perp}\, \frac{\partial\langle T^{+k}_{\text{Bel}}\rangle}{\partial\Delta^j_\perp}\bigg|_{\text{DY}}$$

$$= \Lambda^z \int \frac{\mathrm{d}^2\vec{\Delta}_\perp}{(2\pi)^2}\, e^{-\iota\vec{\Delta}_\perp\cdot\vec{b}_\perp}\left[J(t) + t\,\frac{\mathrm{d}J(t)}{\mathrm{d}t}\right]$$

$$\langle M^z\rangle(b_\perp) = \frac{1}{2}\varepsilon^{3jk}\int \frac{\mathrm{d}^2\vec{\Delta}_\perp}{(2\pi)^2} e^{-\iota\vec{\Delta}_\perp\cdot\vec{b}_\perp}\,\Delta^l_\perp\, \frac{\partial\langle S^{l+k}\rangle}{\partial\Delta^j_\perp}\bigg|_{\text{DY}}$$

$$= -\frac{\Lambda^z}{2}\int \frac{\mathrm{d}^2\vec{\Delta}_\perp}{(2\pi)^2} e^{-\iota\vec{\Delta}_\perp\cdot\vec{b}_\perp}\left[t\,\frac{\mathrm{d}G_A(t)}{\mathrm{d}t}\right]$$

where $J(t) = \frac{1}{2}\left(A(t) + B(t)\right)$

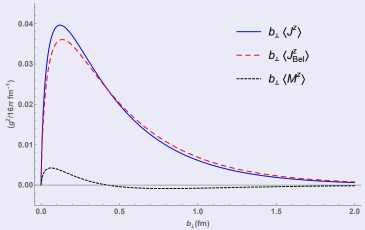

$$\langle J^z\rangle(b_\perp) = \langle J^z_{\text{Bel}}\rangle(b_\perp) + \langle M^z\rangle(b_\perp)$$

Cédric Lorcé et al., Phys. Lett. B 776 (2018) 38-47

Flavor contributions:

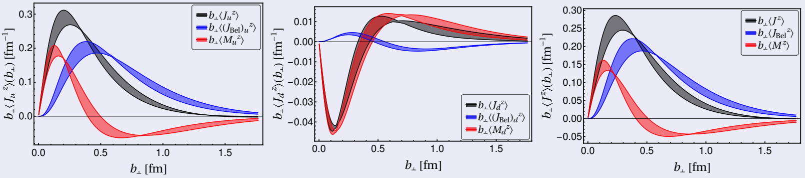

- The "naive" density: defined as the two-dimensional Fourier transform of $J(t)$:

$$\langle J^z_{\text{naive}}\rangle(b_\perp) = \Lambda^z \tilde{J}(b_\perp)$$

by a correction term

$$\langle J^z_{\text{corr}}\rangle(b_\perp) = -\Lambda^z \left[\tilde{L}(b_\perp) + \frac{1}{2} b_\perp \frac{\mathrm{d}\tilde{L}(b_\perp)}{\mathrm{d}b_\perp}\right]$$

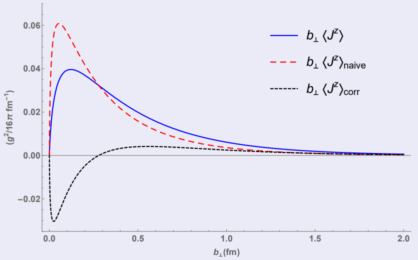

$$\langle J^z\rangle\,(b_\perp) = \langle J^z_{\text{naive}}\rangle(b_\perp) + \langle J^z_{\text{corr}}\rangle(b_\perp)$$

Cédric Lorcé et al., Phys. Lett. B 776 (2018) 38-47

Flavor contributions:

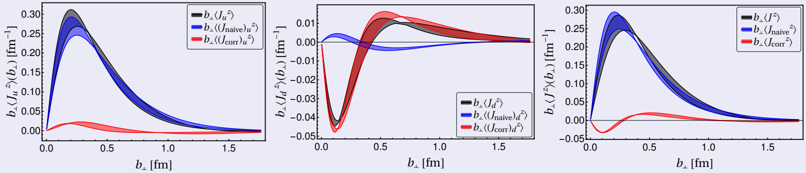

- Monopole and quadrupole contributions to Belinfante-improved TAM:

$$\langle J_{\text{Bel}}^{z(\text{mono})}\rangle(b_\perp) = \frac{\Lambda^z}{3}\left(\tilde{J}(b_\perp) - b_\perp \frac{\mathrm{d}\tilde{J}(b_\perp)}{\mathrm{d}b_\perp}\right)$$

$$\langle J_{\text{Bel}}^{z(\text{quad})}\rangle(b_\perp) = \frac{\Lambda^z}{3}\left(\tilde{J}(b_\perp) + \frac{1}{2} b_\perp \frac{\mathrm{d}\tilde{J}(b_\perp)}{\mathrm{d}b_\perp}\right)$$

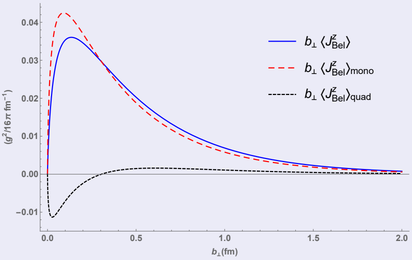

Cédric Lorcé et al., Phys. Lett. B 776 (2018) 38-47

Flavor contributions: